

Elsevier Editorial System(tm) for Tribology International
Manuscript Draft

Manuscript Number: TRIBINT-D-11-00177R1

Title: Identification of a friction model for the bearing channel of hot aluminium extrusion dies by using ball-on-disc tests

Article Type: Full Length Article

Keywords: FE Simulation; Friction model; Hot aluminium extrusion; Bearing channel

Corresponding Author: Dr Liliang Wang,

Corresponding Author's Institution:

First Author: Liliang Wang

Order of Authors: Liliang Wang; Jie Zhou; Jurek Duszczuk ; Laurens Katgerman

Abstract: A physically-based friction model is developed based on the ball-on-disc test results. The model is verified by using double action extrusion tests. Good agreements between the FE predictions and experiments have been obtained, in terms of the extrudate length and steady-state extrusion load, indicating that ball-on-disc test is an effect way of characterizing the friction for the bearing channel of extrusion dies and the nature of friction in the bearing channel can be summarized as a pressure dependant process: formation of isolated adhesive junctions, adhesive junctions growth and coalescence of adhesive junctions.

L. Wang
Department of Materials Science and
Engineering, Delft University of
Technology, Mekelweg 2, 2628 CD
Delft, The Netherlands
E-mail: liliang.wang@imperial.ac.uk

May 15, 2011

Dr. Philippa Cann
Imperial College
Department of Mechanical Engineering,
Tribology Group,
Imperial College,
South Kensington Campus, London, SW7 2AZ, UK,

Dear Dr. Cann,

Enclosed please find the manuscript entitled: *Identification of a friction model for the bearing channel of hot aluminium extrusion dies by using ball-on-disc tests* submitted for publication in Tribology International. The authors are: L. Wang, J. Zhou, J. Duszczyk and L. Katgerman. The basic findings are as follows.

- (1) Short sliding distance ball-on-disc tests can be used to characterize the friction in the bearing channel of the hot aluminium extrusion dies.
- (2) The tribological conditions of hot aluminium extrusion process cannot be reflected by using one single friction testing technique, and a combination of different friction testing techniques should be used. For the bearing channel of the hot aluminium

extrusion dies, the short sliding distance ball-on-disc test is recommended, with the disc made from the workpiece material and ball made from the die material.

- (3) Strong adhesive friction occurs between the hot aluminium and steel and the nature of friction in the bearing channel can be summarized as a pressure dependant process, *i.e.* formation of isolated adhesive junctions, adhesive junctions growth and coalescence of adhesive junctions.

This is an original paper which has neither previously, nor simultaneously, in whole or in part been submitted anywhere else.

Kind regards,

Liliang Wang.

May 15, 2011.

TRIBOLOGY INTERNATIONAL

Statement of Originality

As corresponding author, I Liliang Wang, hereby confirm on behalf of all authors that:

- 1) The paper has not been published previously, that it is not under consideration for publication elsewhere, and that if accepted it will not be published elsewhere in the same form, in English or in any other language, without the written consent of the publisher.
- 2) The paper does not contain material which has been published previously, by the current authors or by others, of which the source is not explicitly cited in the paper.

Research highlights

Ball-on-disc tests can be used to characterize the friction in the bearing channel of aluminium extrusion dies.

The friction in the bearing channel is a pressure dependant process:

At low contact pressure: formation of isolated adhesive junctions

At medium contact pressure: adhesive junctions growth

At high contact pressure: coalescence of adhesive junctions

Yours sincerely,

Liliang Wang (corresponding author), on behalf of the authors

Contact information:

Department of Mechanical Engineering

Imperial College London

Email: Liliang.wang@imperial.ac.uk

Revision notes (TRIBINT-D-11-00177)

Ms. Ref. No.: TRIBINT-D-11-00177

Title: Identification of a friction model for the bearing channel of hot aluminium extrusion dies by using ball-on-disc tests

1. Changes and explanations in response to the comments of Editor

The advice of Editor has been followed and the changes have been made to the manuscript accordingly.

- (1) Please try to improve the English grammar and style throughout the paper.

The advice of Editor has been followed and the paper has been revised carefully and the English grammar and style throughout the paper has been improved.

- (2) The reference listing should conform to the Journal style - see Advice to Authors.

The advice of the editor has been followed and the reference style of Tribology International has been followed.

2. Changes and explanations in response to the comments of Reviewers

The advice of Reviewers has also been followed and the changes have been made to the manuscript accordingly. The added/revised text and explanations are given below.

- (1) The bibliography is primarily focused on simulation tests and critical analysis of them. It lacks a summary review of the results obtained in the literature, the nature of tribological phenomena involved in the hot extrusion of aluminium, and a brief description of the process.

All the three suggestions have been followed and changes were made accordingly.

For the field tests, the friction test results are summarised in Table 1.

For the simulative friction tests, the friction test results are indicated in the text:

“high values of friction coefficients ($1 < \mu < 1.5$) were observed”

“The results obtained from the DAE tests indicate that full sticking friction occurred at the extrudate/die interface when a 15° choke angle was applied in the extrusion dies”

For the tribological tests, the friction test results are indicated in the text:

“The steady-state friction was found to be greater than 1.0 when the testing temperature was higher than 150°C and the magnitude of friction increased with increasing temperature.”

As the reviewers suggested, the nature of tribological phenomena involved in the hot extrusion of aluminium has been reviewed and added into the introduction part, although the fundamental understanding of the friction phenomenon in the bearing channel of hot aluminium extrusion dies is still insufficient.

“In the meanwhile, high values of friction coefficients ($1 < \mu < 1.5$) were observed and this was attributed to a high degree of aluminium to aluminium contact”

“The presence of a continuous transfer layer was thought to be responsible for the high magnitude of the frictional force.”

As the reviewers suggested, a brief introduction of extrusion process has been added into the introduction part:

“Extrusion is a process in which a cast billet of solid metal is converted into a continuous length of generally uniform cross-section by forcing it to flow through a shaped die opening. Generally, the extrusion process is a hot working operation, in which the metal billet is heated to a proper temperature, at which a relatively high ductility and low flow stress can be achieved.”

(2) No friction curves measured from the ball/disc test are presented.

Why? There should be and if so, they should be discussed.

Moreover, the advantage of using a pin on disc test should be more clearly proved.

As the reviewers suggested, the friction curves measured from the ball-on-disc tests are presented (Figure 1 and 5 in the revised manuscript) and the results have been discussed. The ball-on-disc test results have clearly proved the advantage of using a ball-on-disc test, because the friction stresses at different testing temperatures are reasonable and constant. Moreover, the good agreement between the FE simulation results and experimental (DAE) results has proved the advantage of using a ball-on-disc test.

“Figure 1 shows the evolution of the friction coefficient over a sliding distance of 10 laps at different temperatures. It is of interest to note that friction coefficient increases with the sliding distance. At 500 °C, in particular, the friction coefficient increases even by 50%. The increase of the friction coefficient with sliding distance, leads to the uncertainty as to the exact value to be put into FE simulation.”

“Figure 5 shows the evolutions of the calculated shear friction stress at different temperatures and over a sliding distance of 10 laps. It is interesting to see that the shear friction stress starts from a relatively low value, and then becomes stable at different temperatures, while the friction coefficient increases considerably (Figure 1). The low shear friction stress at the initial stage may be due to the oxide layer on the disc and ball surfaces, which tends to lower the adhesion between aluminium and steel. After the initial stage of sliding, the oxide layer may be broken up and metal-to-metal contact occurs, leading to the increases in friction stress. In addition, the severe plastic deformation on the surface material may generate a considerable work-hardening effect, which may also lead to the rise of shear friction stress.”

(3)p. 9, line 43: specify the distance of sliding.

The reviewers' suggestion has been followed and the sliding distance (1, 5 and 10 laps of sliding) has been specified in the text.

(4)p. 13, line 29: clarify what is meant by "transition from a slippery patch and adhesive zone"

The reviewers' suggestion has been followed and the explanation and the microstructure of a transition zone have been added into the manuscript:

“At this stage, an in-continuous tribo-layer might be visible on the die land, and the so-called transition zone between the slipping and sticking zone may be observed, as shown in Figure 6 (b) and (c). According to, the transition zone is normally observed when extruding with low die temperatures, and this region is composed of a sportlike aluminium deposit.”

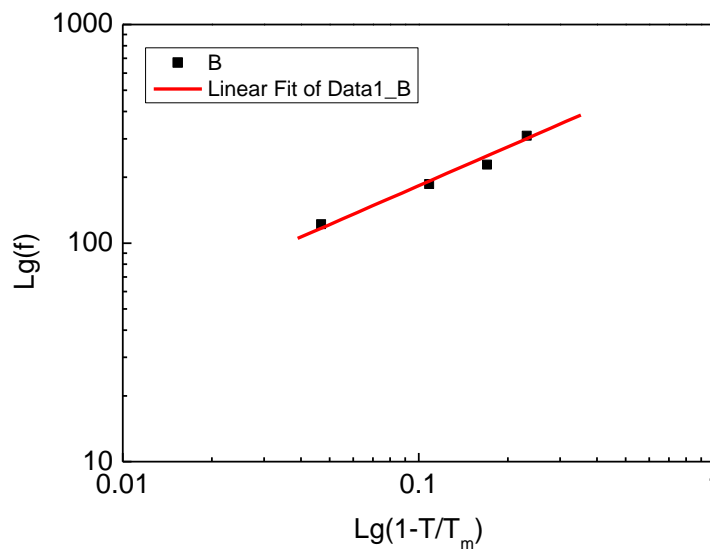
(5)p. 13, line 34: the authors describe a mechanism of coalescence of junctions (does it occur at the entrance of the die?) accompanied by the formation of a continuous transfer layer (is this layer homogeneous?).

Yes, the coalescence of adhesive junctions occurs at the entrance of the extrusion die, because the contact pressure in this region is much higher compared to that of the other regions in the extrusion die. This layer is a continuous layer and is homogeneous. The microstructure of the worn extrusion die (Figure 6 in the revised manuscript) shows that the worn die surface in the sticking zone is very smooth,

suggesting that a homogeneous layer of surface material has been removed by the extrudate.

- (6)p.14: the authors should justify the physical origin of a power law to model the resistance of the junction in equation 6.

The physical origin of the power law is indicated in the figure shown below. In this figure, the friction stresses and temperature are both plotted in the Log scale, and a liner fitting can fit the experimental data very well, then we normally select a power law in the model.



- (7) What conclusions the authors can draw from the calculations presented in Figure 6. The latter are not exploited. Why?

Figure 6 shows the FE model used in the present research. The simulation results were not exploited explicitly, but presented in Figures 10-13 in terms of the extrudate lengths and extrusion loads. The results obtained from the FE model shown in Figure 6 has led to the conclusions that the proposed physically based friction model can be used to model the friction in the bearing channel of hot extrusion dies.

- (8) The authors observed a correlation between the length of the bearing area and the possibility of growth of the area of contact (and friction). They should clarify the interpretation. Is it connected to the possibility of junctions to be formed?

In the current research, choked dies with 15' die angle were used to apply contact pressure to the extrudates and full sticking friction was observed in all the DAE tests

conducted in the present research. In the manuscript, the correlation between the length of the extrudates and bearing area has been explained:

“The length difference of the extrudates increases with increasing ram displacement. At the initial stage of the DAE, the workpiece is extruded at the same extrusion speed in both of the dies. As the ram displacement increases, the friction force increases at the same rate in the two dies due to the increasing contact area. When the extrudate lengths are greater than 2 mm, the contact area in the 2 mm bearing cannot be further increased. Thus a constant friction force is achieved in the 2 mm bearing. In the 6 mm bearing, however, the contact area is further increased due to the increase of the extrudate length, thus the friction force increases and the material flow in the 6 mm bearing is restricted, consequently the extrusion speed slows down. In the meanwhile, the rate-dependant property of the billet material becomes explicit. In the severe deformation zone of the 2 mm bearing, the material is enhanced due to the higher extrusion speed and becomes more difficult to be deformed. In the severe deformation zone of the 6 mm bearing, however, the low extrusion speed results in lower material strength, thus the material becomes easier to be extruded. As such, a dynamic balance is maintained throughout the DAE process: the friction between extrudates and bearing surfaces increases the length difference of the extrudates; on the other hand, the effect of rate-dependent material behaviour decreases the length difference.”

(9) Pictures of worn surfaces that correspond to different stages the model ASFM should be shown. This would allow the author to demonstrate more clearly the validity of their model.

The reviewers’ suggestion has been followed and the microstructures of worn surfaces that correspond to different zones in the extrusion die have been added into the manuscript (Figure 6 in the revised manuscript).

The authors sincerely thank the reviewers for their contributions to the improvement of the manuscript and for sharing their thoughts.

1
2
3
4 **Identification of a friction model for the bearing channel of hot**
5
6
7 **aluminium extrusion dies by using ball-on-disc tests**
8
9

10
11
12 Liliang Wang*, Jie Zhou, Jurek Duszczuk and Laurens Katgerman
13
14

15
16
17 *Department of Materials Science and Engineering, Delft University of Technology,*
18
19
20 *Mekelweg 2, 2628 CD Delft, The Netherlands*
21
22
23

24
25 **Abstract**
26
27

28
29
30 A physically-based friction model is developed based on the ball-on-disc test results. The
31
32 model is verified by using double action extrusion tests. Good agreements between the
33
34 FE predictions and experiments have been obtained, in terms of the extrudate length and
35
36 steady-state extrusion load, indicating that ball-on-disc test is an effect way of
37
38 characterizing the friction for the bearing channel of extrusion dies and the nature of
39
40 friction in the bearing channel can be summarized as a pressure dependant process:
41
42 formation of isolated adhesive junctions, adhesive junctions growth and coalescence of
43
44 adhesive junctions.
45
46
47
48
49
50

51
52 *Keywords:* FE Simulation; Friction model; Hot aluminium extrusion; Bearing channel
53
54
55

56 * Corresponding author.
57

58
59 E-mail address: Liliang.wang@gmail.com
60
61

1
2
3
4
5
6
7
8
9 **1. Introduction**

10 FE simulation of the extrusion processes is widely used in both scientific research and
11 industrial practice. The selection of friction models and the assignment of friction
12 coefficients or factors for the FE simulations of extrusion processes remain an essential
13 issue, because the accuracy of the simulation results is strongly affected by the flow
14 stress of workpiece material (thermo-viscoplastic behavior at elevated temperatures) and
15 the assignment of boundary conditions, *e.g.* friction boundary conditions. The uncertainty
16 of flow stress is low when the constitutive equations determined from thermo-mechanical
17 testing are implemented. However, unreliable FE simulation results could be obtained if
18 the friction boundary conditions are not assigned correctly.
19
20
21
22
23
24
25
26
27
28
29
30
31
32
33
34
35
36
37

38 Hot aluminium extrusion is a complex thermo-mechanical process, which involves highly
39 complicated chemical and tribological interactions between the workpiece and tooling. It
40 was found that many practical problems in the hot extrusion industry, such as wear of the
41 extrusion dies [1-4], surface quality of the extruded profiles [5], die lines and pick up [6]
42 *etc.*, are related to the strong adhesion between the hot aluminium and the die due to
43 strong chemical and atomic interactions between hot aluminium and steel, which is the
44 main reason for the excessively high friction observed during hot aluminium extrusion
45 [1-3, 7].
46
47
48
49
50
51
52
53
54
55
56
57
58
59
60
61
62
63
64
65

1
2
3
4 In the past years, efforts have been made to study the tribological phenomenon of the
5
6 extrusion process and the developed friction testing techniques can be classified as three
7
8 different groups, namely, field tests; simulative tests (or physical simulation tests) and
9
10 tribological tests.
11

12
13
14
15
16 In general, field test is to estimate the friction coefficient or factor by using extrusion
17
18 friction tests. According to the material flow response to the friction force, some novel
19
20 extrusion friction tests have been developed, including double backward extrusion [8],
21
22 combined forward rod-backward can extrusion [9] and combined forward conical /
23
24 straight can-backward straight can extrusion [10]. These tests were designed with
25
26 highlighted friction sensitivity in extrudate lengths. Lubricants can be evaluated and the
27
28 global friction coefficient or factor on the workpiece/tooling interface can be determined
29
30 quantitatively with the aid of FE simulations. In addition, the friction sensitivity of
31
32 extrusion load [11, 12] was used for friction characterization, in which the average
33
34 friction over the container wall was estimated. For the regions of particular interest,
35
36 specialized techniques are employed. For instance, the direct stress measurement
37
38 techniques, *e.g.* stress transmitting pins [13] have been used to measure the pressure
39
40 distribution on the die face during hot aluminium extrusion. Extrusion friction tests for
41
42 extrudate/bearing interface [4, 14, 15] was used to characterize friction in the bearing
43
44 channel of extrusion dies, in which a transition from full sticking to sliding was
45
46 experimentally observed and the friction coefficients were therefore determined from the
47
48 lengths of sticking and sliding zones [14-16].
49
50
51
52
53
54
55
56
57
58
59
60
61
62
63
64
65

1
2
3
4 Field tests are normally time consuming, expensive and difficult to control. In most of the
5
6 field tests, the local contact conditions vary significantly throughout the whole operating
7
8 cycle, and the individual effect of each factor is rather difficult to be discriminated.
9
10 Therefore, there is a need for simplified friction testing techniques, in which, more stable
11
12 contact conditions can be achieved. Hence, simulative tests have been proposed and
13
14 conducted. The block on cylinder tests [1, 7] were developed to simulate the contact
15
16 between the workpiece and extrusion die, and the wear mechanisms in the bearing
17
18 channel region were studied. The results revealed that adhesive wear and abrasive wear
19
20 were dominant wear patterns of the extrusion dies. In the meanwhile, due to the strong
21
22 chemical bonding between the hot aluminium and steel, high friction coefficients were
23
24 observed. Most recently, a novel simulative friction test method highlighting the friction
25
26 in the bearing channel of the die, double action extrusion (DAE), was developed [17, 18].
27
28 In the DAE, an aluminium billet was pressed against two extrusion dies with different
29
30 bearing lengths and two indirect extrusions took place simultaneously. The lengths of the
31
32 extrudates were found to be highly friction sensitive due to different friction in the two
33
34 dies, and thus the friction between the extrudate and bearing channel of the die during hot
35
36 aluminium extrusion can be characterized.
37
38
39
40
41
42
43
44
45
46
47

48 In the field tests or simulative tests, it is rather difficult to study the effects of individual
49
50 factor, such as temperature, sliding speed and contact pressure *etc.*, on the friction. The
51
52 tribological test is a sensible technique to understand the physical fundamentals of the
53
54 friction under hot aluminium extrusion conditions. In the past, tribological tests (pin/ball-
55
56 on-disc tests) have been employed to identify the friction coefficients for metal cutting
57
58
59
60
61
62
63
64
65

1
2
3
4 process [19-22]. Recently, the first attempt to determine the friction coefficient for hot
5
6 aluminium extrusion process by using ball/pin-on-disc tests has been conducted [23, 24].
7
8
9 However, the tribological test results have not been implemented into the FE simulations
10
11 of hot aluminium extrusion yet, probably due to the lack of knowledge about the
12
13 evolution of the contact interface during ball-on-disc tests.
14
15
16
17
18

19 The aim of this research is to understand the fundamental of friction phenomenon in the
20
21 bearing channel of the extrusion die from a tribological point of view. Moreover, based
22
23 on the ball-on-disc test results, a physically-based friction model has been developed and
24
25 implemented into the simulation of hot aluminium extrusion process.
26
27
28
29
30

31 **2. Selection of friction testing techniques for the friction characterization of hot** 32 **aluminium extrusion processes** 33 34 35 36 37

38 During the friction tests, the large variety of contact conditions, such as temperature,
39
40 contact pressure, sliding distance, sliding velocity and oxidation scale should be
41
42 considered very carefully [25], because these factors influence the friction coefficients
43
44 considerably. In general, it is very unlikely to emulate all the contact conditions or reflect
45
46 all the tribological conditions by using one single friction testing technique, because one
47
48 friction testing technique is only able to reflect one specific or a few tribological
49
50 conditions, *i.e.* the tribological conditions of a particular region of the workpiece / tooling
51
52 interface. Therefore, in order to characterize the friction of extrusion processes, a
53
54 combination of different testing methods should be used, for instance, the combination of
55
56 extrusion friction tests (to determine the friction between the billet and container) and
57
58
59
60
61
62
63
64
65

1
2
3
4 short sliding distance ball-on-disc tests (to determine the friction of the bearing channel
5
6 region).
7
8
9

10
11 The extrusion friction tests were developed to estimate the global friction coefficient at
12 the billet/container interface. During the tests, high contact pressure and intensive surface
13 enlargement can be achieved [9, 10, 12, 26, 27]. Most recent research results have shown
14 that different contact conditions in the extrusion friction tests can be achieved by
15 adjusting the extrusion ratio[27]: low contact pressure and surface enlargement can be
16 achieved when low extrusion ratio is used, thus a high friction sensitivity can be obtained.
17
18 If a high extrusion ratio is used, high contact pressure and surface enlargement are
19 obtained, which resemble the real contact condition of forging or extrusion processes, but
20 sacrifice the friction sensitivity. The combination of extrusion friction tests and FEM
21 simulations is an effective way of estimating global friction at the billet and container
22 interface.
23
24
25
26
27
28
29
30
31
32
33
34
35
36
37
38
39
40

41 Ball/pin-on-disc test is a widely used laboratory testing technique for the quantitative
42 study of tribological behavior of materials. During ball-on-disc tests, a high contact
43 pressure can be achieved in a small contact area between the ball and the rotating disc. If
44 a soft material is sliding over a harder one, severe plastic deformation may occur, which
45 could lead to the removal of oxide layers and the contact of pure metals. In the
46 meanwhile, the contact pressure may drop with the increasing sliding distance. Therefore,
47 ball-on-disc tests are favorable to the friction characterization of the regions, in which
48 local contact pressure is high and new surface generation is severe, such as the bearing
49
50
51
52
53
54
55
56
57
58
59
60
61
62
63
64
65

1
2
3
4 channel of hot aluminium extrusion dies. During hot aluminium extrusion, fresh
5
6 aluminium is extruded from the container, and in the die bearing, a pure metal contact
7
8 takes place. It is well known that the presence of chemical stable surface oxides or scale
9
10 prevents the strong atomic interactions [28]. Therefore, in order to reproduce the friction
11
12 conditions in the bearing channel, it is vital to choose a friction testing technique being
13
14 able to remove the surface oxides. Obviously, short sliding distance ball-on-disc test is
15
16 one of the best friction testing techniques over the other ones, because during the ball-on-
17
18 disc tests, severe plastic deformation occurs at the ball / disc interface [19, 20, 23],
19
20 especially during the run-in period. Short sliding distance ball-on-disc test is highly
21
22 suitable for the study of the friction between fresh metals, which emulates the contact
23
24 condition in the bearing channel or welding chamber of the extrusion dies. However, the
25
26 friction test results obtained from ball-on-disc tests cannot be transferred into FE
27
28 simulations of extrusion processes directly as the friction boundary conditions, due to the
29
30 complicated nature of the evolution of contact conditions during the tests. Therefore, the
31
32 selection of testing parameters, such as pin and disc materials, sliding distance and size of
33
34 the ball has to be considered carefully. Furthermore, friction data processing has to be
35
36 conducted through FEM simulation or theoretical analysis.
37
38
39
40
41
42
43
44
45
46
47

48 The selection of the pin and disc materials affects ball-on-disc test results. If the pin is
49
50 made from a soft material, and the disc is made from a hard one, severe plastic
51
52 deformation and wear would occur on the tip of the pin, which leads to a significant
53
54 enlargement of the contact area. After the run-in period, a steep decrease of contact
55
56 pressure occurs and the contact pressure during the steady-state sliding is close to the
57
58
59
60
61
62
63
64
65

1
2
3
4 yield strength of the soft material. On the other hand, if the disc is made from a soft
5
6 material, while the pin is made from a hard one, plastic deformation tends to occur in the
7
8 disc, but the material flow is most likely constrained by the remainder disc material,
9
10 which is much larger than the size of the wear track. Hence a relatively high hydrostatic
11
12 pressure which is greater than the strength of the disc material would be imposed onto the
13
14 spherical pin head. Therefore, different materials combinations would result in different
15
16 contact pressures, and the selection of pin and disc mating materials need to be
17
18 considered carefully prior to testing, especially when the strengths of the pin and disc
19
20 materials are different. In the meanwhile, the selection of ball size and sliding distance is
21
22 of great importance. In general, the contact pressure increases with decreasing ball size
23
24 [29] and decreases with increasing sliding distance [30].
25
26
27
28
29
30
31

32
33 When a hard pin is sliding over a soft disc, the apparent friction coefficient obtained from
34
35 the test is normally composed of plowing and shearing (adhesive) friction [20, 21, 31].
36
37 The plowing friction is caused by the plastic deformation of the disc material in front of
38
39 the pin, which depends on the size of the ball, sliding distance and the material strength.
40
41 Consequently, the test results cannot be transferred into a metal forming operation
42
43 directly, because the existence of plowing friction leads to an overestimation of the
44
45 friction between the mating materials. The plowing and shear friction have to be
46
47 discriminated by means of FEM simulations [20, 21] or theoretical analysis [24, 32], and
48
49 only the shear component of apparent friction representing the real friction between the
50
51 two mating materials should be used in the FE simulations of metal forming operations as
52
53 boundary conditions [20, 21]. However, when the material combination of soft pin and
54
55
56
57
58
59
60
61
62
63
64
65

1
2
3
4 hard disc is used, the friction coefficients obtained from the tests are mainly attributed to
5
6 the shearing (adhesive) friction. Therefore, with the knowledge about the contact pressure
7
8 evolution, the results can be transferred into the FE simulations as friction boundary
9
10 conditions. To simulate the tribological conditions in the bearing channel of the hot
11
12 aluminium extrusion die, the short sliding distance ball-on-disc test is recommended,
13
14 with the disc made from the workpiece material and ball made from the die material.
15
16
17
18
19
20

21 **3. Determination of friction coefficient for the bearing channel of hot** 22 **aluminium extrusion dies by using ball-on-disc tests** 23 24 25 26 27

28 A CSM® high-temperature tribometer with a ball-on-disc configuration was used for the
29
30 friction characterization. To emulate the extrusion process, the disc was made from
31
32 AA7475 aluminium alloy, which was the same as the billet material used in the extrusion
33
34 tests. The hardened H11 steel was selected as the mating material, which was the same
35
36 material as that of extrusion dies. The tests were carried out under a constant normal load
37
38 of 6 N at 350, 400, 450 and 500°C [24]. In order to achieve a high contact pressure
39
40 between the mating materials, short sliding distance ball-on-disc tests were employed to
41
42 represent the friction condition of the bearing channel of the hot aluminium extrusion
43
44 process. The friction coefficients between AA7475 and H11 steel were determined.
45
46
47
48
49
50
51

52 In order to transfer the friction test results of ball-on-disc tests into FE simulations as
53
54 friction boundary conditions, it is of great importance to understand the evolution of the
55
56 contact conditions during the tests. A previously developed model being able to
57
58 characterize the evolution of contact interface during high-temperature ball-on-disc tests
59
60
61
62
63
64
65

was used to determine the mean friction stresses at different temperatures [24], which will be used for friction modelling in this research.

Figure 1 shows the forces acting on an elemental area during ball-on-disc testing, which are given in Equation (1).

$$\begin{cases} dF_x = \left(pr^2 \sin^2 \beta \cos \gamma + fr^2 \sin \beta \sqrt{\cos^2 \gamma \cos^2 \beta + \sin^2 \gamma} \right) d\gamma d\beta \\ dF_z = \left(pr^2 \cos \beta \sin \beta - fr^2 \frac{\cos \gamma \sin^2 \beta \cos \beta}{\sqrt{\cos^2 \gamma \cos^2 \beta + \sin^2 \gamma}} \right) d\gamma d\beta \end{cases} \quad (1)$$

First lap of wear

The aluminium disc was assumed to behave as a viscoplastic material at elevated temperatures and the elastic recovery of the disc at the rare part of the ball was omitted.

Figure 2 schematically shows the contact interface during the 1st lap of wear. Equation (2) can be used to calculate the tangential and normal forces acting on the ball surface.

$$\begin{cases} F_x = 2 \int_0^{\xi_1} \int_0^{\pi/2} dF_x \\ F_z = 2 \int_0^{\xi_1} \int_0^{\pi/2} dF_z \end{cases} \quad (2)$$

where ξ_1 is the upper integral limit of angle β (see Figure 2a where W_1 is the width of the wear track after the first lap of wear).

Arbitrary (i+1)th lap of wear

The contact interface of an arbitrary lap of wear is schematically shown in Figure 3. The tangential and normal forces acting on the ball can be calculated by Equation (3).

$$\begin{cases} F_x = 2 \int_0^{f_i(\gamma)} \int_0^{\pi/2-\omega_i} dF_x + 2 \int_0^{\xi_i} \int_{\pi/2-\omega_i}^{\pi/2} dF_x \\ F_z = 2 \int_0^{f_i(\gamma)} \int_0^{\pi/2-\omega_i} dF_z + 2 \int_0^{\xi_i} \int_{\pi/2-\omega_i}^{\pi/2} dF_z \end{cases} \quad (3)$$

As shown in Figure 3b, in the area *COD*, $f_i(\gamma)$ is the upper integral limit of β , and in the areas *AOD* and *COB*, ξ_i is the upper integral limit of angle β . ω_i is the angle for locating the position of the front contact boundary during the $(i+1)$ th lap of wear.

To determine the constants in the model, three tests with different wear laps (1, 5 and 10 laps) were conducted at each temperature. The friction coefficient was continuously recorded during the test. Thereafter, wear tracks were examined using an optical microscope. The average width of the wear track in each lap was determined from 12 measurements.

4. A physically-based adhesive strength friction model (ASFM) for the bearing channel of hot aluminium extrusion die

According to the classic theory of tribology, the friction force mainly stems from ploughing (due to hard asperities and trapped wear debris) and adhesive (due to atomic or chemical interactions) forces [33-35]. At elevated temperatures, the adhesive friction plays a dominant role, due to the strong atomic or chemical interactions, especially under

1
2
3
4 high contact pressures [1-3, 36]. This is mainly due to the following reasons: at elevated
5
6 temperatures, the atoms in both materials in contact are highly activated, which aids the
7
8 interdiffusion at the surface layers of the materials and a strong chemical bonding tends
9
10 to be established. The mating materials and surface oxides are relatively soft and easy to
11
12 be deformed or penetrated, which thus leads to the contact of pure metals. In addition, the
13
14 high contact pressure (several times greater than the flow stress of the workpiece material)
15
16 further aids the severe plastic deformation of the asperities or oxidation scale, and brings
17
18 the faying material highly close to each other to a distance of atomic level. Therefore, in
19
20 the bearing channel of hot aluminum extrusion, the strong chemical or diffusion bonding
21
22 is the dominant friction mechanism, which has been verified experimentally before [2, 3].
23
24 Also, the strong interactions between hot Al and steel have been observed in the forge
25
26 welding process [37-39]. From a micro-scale point of view, the influence of the contact
27
28 pressure is to change the real contact area, *i.e.* the number of asperities in contact.
29
30 Therefore, the nature of different friction modes within the bearing channel could be
31
32 summarized as:
33
34
35
36
37
38
39
40
41
42

43 Formation of isolated adhesive junctions → Adhesive junctions growth → Coalescence
44
45 of adhesive junctions.
46
47
48
49

50 *Formation of isolated adhesive junctions.* At low contact pressure conditions, strong
51
52 adhesion occurs on the tips of plastically deformed asperities, but the faying surfaces are
53
54 only supported by a small number of asperities, thus only a few isolated adhesive
55
56 junctions are formed and normally too small to be observed by naked eyes. At this stage,
57
58
59
60
61
62
63
64
65

1
2
3
4 no adhesive layers can be observed. Therefore a so-called slipping zone is experimentally
5
6 observed.
7
8
9

10
11 *Adhesive junctions growth.* As the increase of contact pressure, the number of plastically
12 deformed asperities is increased, to support the increased contact pressure. In some
13 regions with a higher asperity density, adhesive junctions growth takes place due to the
14 plastic deformation and some of the adhesive junctions may coalesce to each other
15 locally. Consequently, the workpiece material or intermetallic wear debris could adhere
16 to the bearing surface of the die, due to the strong adhesive bonding. At this stage, an in-
17 continuous tribo-layer might be visible on the die land, and the so-called transition zone
18 between the slipping and sticking zone can be observed.
19
20
21
22
23
24
25
26
27
28
29
30

31
32
33 *Coalescence of adhesive junctions.* At the die entrance, where a high contact pressure is
34 achieved, the real contact area is maximized, thus the number of adhesive junctions is
35 significantly increased and they are close to each other, thus tend to coalesce with each
36 other. Moreover, a great amount of workpiece material may transfer from the extrudates
37 to the bearing surface of the die, due to the strong adhesive bonding. Therefore there
38 exists a great chance for the adhesive junctions within a large area to coalesce with each
39 other and thus the adhesive junctions can be observed by naked eyes. At this stage, a
40 continuous tribo-layer, *i.e.* the so-called adhesive zones, can be observed on the bearing
41 surface. However, after extrusion, the inlet of the bearing is heavily worn and a
42 continuous tribo-layer may not be observed. This is probably due to the high rate of
43 material renewal at the inlet of the bearing channel [2].
44
45
46
47
48
49
50
51
52
53
54
55
56
57
58
59
60
61
62
63
64
65

1
2
3
4
5
6
7 In this research, the strong adhesive friction generated from pure metal contact is
8
9 modelled, and the strength of adhesive junctions is considered to be determined by two
10
11 factors, namely, the rate of atomic interaction and the strength of adhesive joints
12
13 (Equation 6). The interaction rate at atomic level increases with increasing temperature,
14
15 which can be modeled by using an Arrhenius type equation [40] (Equation 7). The
16
17 bonding strength decreases with increasing temperature, due to the decrease of the
18
19 strength of adhesive joints with increasing temperatures, and the bonding strength drops
20
21 to zero at the melting temperature of AA7475 (Equation 6). The friction stresses obtained
22
23 from short sliding distance ball-on-disc tests, details found in [24], were used to
24
25 determine the constants of the model, by fitting the outputs of the model with the stress-
26
27 temperature curve obtained from ball-on-disc tests. Table 1 lists the determined material
28
29 constants. As can be seen from Figure 4, a good agreement between the model and
30
31 experimental results was obtained.
32
33
34
35
36
37
38
39
40

$$f(T) = \tau_0 D \left(1 - \frac{T}{T_m}\right)^n \quad (6)$$

$$D = D_0 \cdot \exp\left(-\frac{Q}{RT}\right) \quad (7)$$

41
42
43
44
45
46
47
48
49
50
51
52 where $f(T)$ is temperature dependant bonding strength or friction stress in a unit area;
53
54

55 τ_0 is the mean adhesive strength at room temperature (300 K) in a unit area;
56

57 D is the inter-diffusion coefficient at elevated temperatures;
58

59 T is the mean contact temperature (K);
60
61
62
63
64
65

1
2
3
4 T_m is the melting temperature of the workpiece material (K);
5
6

7 Q is the activation energy;
8
9

10 R is the universal gas constant;
11

12 D_0 and n are constants;
13
14

15
16
17 Table 1 Material constants of the ASFM for hot AA7475 and H11 steel
18

$\tau_0 (MPa)$	$T_m (K)$	$Q (J/mol)$	$R (J/K/mol)$	D_0	n
378	811	2400	8.314	3.62	0.7

19
20
21
22
23
24
25
26
27 In this model, the bonding strength is determined by the combined effects of atomic
28 interaction and the strength of adhesive joints, with the assumption that pure metal
29 contact is taking place. At low temperature conditions ($T < 0.5T_m$ approximately), the
30 interdiffusion rate increases with the increasing temperature. At this stage, the increase of
31 temperature does not affect material strength significantly. Therefore the increase of
32 inter-diffusion rate plays a dominant role under the low temperature circumstances, thus
33 an increasing adhesive strength is predicted. The maximum value of adhesive strength is
34 achieved at about 423 K ($0.5T_m$ approximately). At high temperatures ($0.5T_m < T \leq T_m$),
35 the bonding strength decreases with increasing temperature, because the drop of the
36 strength of adhesive joints plays a dominant role, although the atoms are highly activated
37 and atomic interactions are more intensive. Therefore a decreased adhesive strength with
38 the increasing temperature can be observed, which is consistent with other research
39 results [35, 41].
40
41
42
43
44
45
46
47
48
49
50
51
52
53
54
55
56
57
58
59
60
61
62
63
64
65

5. Verification of the friction model

5.1. Experiment and FE simulation details

The double action extrusion (DAE) tests [17, 42], highlighting the friction in the bearing channel of the extrusion dies, were used to verify the proposed friction model. Figure 5 (a) shows the principle of the DAE, which was conducted on a Gleeble 3800 material thermo-mechanical simulator and Figure 5 (b) shows the experimental setup. In the tests, the combination of 2 and 6 mm bearing dies was employed to maximize the effect of friction in the bearing channels [18]. It has been found that the DAE is highly sensitive to the friction in the bearing regions, in terms of extrudate lengths and steady-state extrusion load. Figure 5 (c) shows the typical test results of DAE and the length differences were caused by the different friction forces generated from the two different extrusion dies, with different bearing lengths used. Figure 5 (d) shows the typical extrusion forces of DAE tests at different testing temperatures. As can be seen from Figure 5 (d), the extrusion forces decreased with increasing temperature, mainly due to the decreasing strength of the workpiece material with rising temperature. The extrusion forces at these temperatures showed a similar trend, *i.e.* a small plateau at the very early stage, followed by a sharp increase in extrusion force and then a gentle decrease as the process proceeded further. The small plateau corresponds to the initiation of extrusion toward both of the die (upsetting) and the sharp force increase corresponds to breakthrough. In DAE, there is no friction between the billet and container and therefore the extrusion force in the steady state reflects the dynamic balance of the deformation force of the workpiece material and the friction forces in the two dies which are governed by temperature and influenced by the temperature evolution during DAE.

1
2
3
4
5
6
7 DEFORM 3D version 6.1 was used to simulate the DAE process. Figure 6 shows the
8
9 FEM model of the DAE. All the objects in the model were meshed with tetrahedral
10
11 elements. The flow stress data of AA7475 aluminium alloy were determined from hot
12
13 compression tests on a Gleeble 3800 material thermomechanical simulator, under a wide
14
15 range of strain rate (0.01-180 s⁻¹), with the data at high strain rates corrected for
16
17 deformational heating [43]. The ASFMs were implemented into DEFORM 3D V6.1 via
18
19 user defined subroutine. In DEFORM, to avoid the overestimation of friction stress, the
20
21 value of the friction stress calculated from the a friction model is compared with the shear
22
23 flow stress of the deformed material at each iteration step and automatically changed to
24
25 the shear flow stress, if the calculated friction stress is larger than the shear flow stress.
26
27
28
29
30
31
32

33 **5.2. Friction model verification by DAE tests**

34
35
36
37

38
39 Figures 7-9 show the comparisons in the lengths of the extrudates between the DAE
40
41 experiments and FEM simulations. In these figures, the FEM predictions of the extrudate
42
43 lengths with the use of ASFMs are superimposed onto the experimental data. At different
44
45 temperatures, the extrudates from the 2 mm bearing are longer than those from the 6 mm
46
47 bearing. The length difference of the extrudates increases with increasing ram
48
49 displacement. At the initial stage of the DAE process, the workpiece is extruded at the
50
51 same extrusion speed in both of the dies. As the ram displacement increases, the friction
52
53 force increases at the same rate in the two dies due to the increasing contact area. When
54
55 the extrudate lengths are greater than 2 mm, the contact area in the 2 mm bearing cannot
56
57
58
59
60
61
62
63
64
65

1
2
3
4 be further increased. Thus a constant friction force is achieved in the 2 mm bearing. In
5
6 the 6 mm bearing, however, the contact area is further increased due to the increase of the
7
8 extrudate length, thus the friction force increases and the material flow in the 6 mm
9
10 bearing is restricted, consequently the extrusion speed slows down. In the meanwhile, the
11
12 rate-dependant property of the billet material becomes explicit. In the severe deformation
13
14 zone of the 2 mm bearing, the material is enhanced due to the higher extrusion speed and
15
16 becomes more difficult to be deformed. In the severe deformation zone of the 6 mm
17
18 bearing, however, the low extrusion speed results in lower material strength, thus the
19
20 material becomes easier to be extruded. As such, a dynamic balance is maintained
21
22 throughout the DAE process: the friction between the extrudates and bearing surfaces
23
24 increases the length difference of the extrudates; on the other hand, the effect of rate-
25
26 dependent material behaviour decreases the length difference. As can be seen from the
27
28 figures, at these three extrusion temperatures, the implementation of the ASFM has led to
29
30 highly accurate predictions, in terms of the extrudate lengths, suggesting that the ASFM
31
32 is able to represent the friction conditions at the extrudate/bearing interface.
33
34
35
36
37
38
39
40
41
42

43 Figure 10 shows the FEM predicted and experimentally obtained steady-state extrusion
44
45 forces at different extrusion temperatures. The extrusion force decreases with increasing
46
47 temperature due to the material softening at higher temperatures. It can be seen that
48
49 predictions from the ASFM show the same trend as the experimental results in terms of
50
51 the temperature effect on the extrusion force. The predictions from the ASFM achieved a
52
53 very good agreement between the FE predictions and experimental results.
54
55
56
57
58
59
60
61
62
63
64
65

1
2
3
4
5
6 **6. Conclusions**
7
8
9

10 In this study, a physically based friction model (ASFM) was developed and implemented
11 into the FE simulation of hot aluminium extrusion process. Good agreements between the
12 FE simulations and experiments were achieved, in terms of extrudate length and steady
13 state extrusion force, indicating that ball-on-disc tests can represent the friction
14 conditions in the bearing channel of the hot aluminium extrusion dies. The tribological
15 conditions of hot aluminium extrusion process cannot be reflected by using one single
16 friction testing technique, and a combination of different friction testing techniques
17 should be used. For the bearing channel of the hot aluminium extrusion dies, the short
18 sliding distance ball-on-disc test is recommended, with the disc made from the workpiece
19 material and ball made from the die material. Strong adhesive friction occurs between the
20 hot aluminium and steel and the nature of friction in the bearing channel can be
21 summarized as a pressure dependant process, *i.e.* formation of isolated adhesive junctions,
22 adhesive junctions growth and coalescence of adhesive junctions.
23
24
25
26
27
28
29
30
31
32
33
34
35
36
37
38
39
40
41
42
43
44

45 **References**
46
47

- 48 1 Björk, T., Bergstrom, J. and Hogmark, S. Tribological simulation of aluminum
49 hot extrusion. *Wear*, 1999, 224(2), 216-225.
50
51 2 Björk, T., Westergård, R. and Hogmark, S. Wear of surface treated dies for
52 aluminium extrusion -- a case study. *Wear*, 2001, 249(3-4), 316-323.
53
54 3 Gutovskaya, J., Solberg, J.K., Lange, H.I. and Andersen, L.H. Wear of Inconel
55 718 die during aluminium extrusion--a case study. *Wear*, 2004, 256(1-2), 126-132.
56
57 4 Saha, P.K. Thermodynamics and tribology in aluminum extrusion. *Wear*, 1998,
58 218(2), 179-190.
59
60
61
62
63
64
65

- 1
2
3
4 5 Ma, X., De Rooij, M.B. and Schipper, D.J. Modelling of contact and friction in
6 aluminium extrusion. *Tribology International*, 2010, 43(5-6), 1138-1144.
7
8 6 Clode, M.P. and Sheppard, T. Formation of die lines during extrusion of AA6063.
9 *Materials Science and Technology*, 1990, 6(8), 755-763.
10
11 7 Tercelj, M., Smolej, A., Fajfar, P. and Turk, R. Laboratory assessment of wear on
12 nitrided surfaces of dies for hot extrusion of aluminium. *Tribology International*, 2007,
13 40(2), 374-384.
14
15 8 Buschhausen, A., Weinmann, K., Lee, J.Y. and Altan, T. Evaluation of lubrication
16 and friction in cold forging using a double backward-extrusion process. *Journal of*
17 *materials processing technology*, 1992, 33(1-2), 95-108.
18
19 9 Nakamura, T., Bay, N. and Zhang, Z.L. FEM simulation of friction testing
20 method based on combined forward rod-backward can extrusion. *Journal of Tribology-*
21 *Transactions of the Asme*, 1997, 119(3), 501-506.
22
23 10 Nakamura, T., Bay, N. and Zhang, Z.L. FEM simulation of a friction testing
24 method based on combined forward conical can-backward straight can extrusion. *Journal*
25 *of Tribology-Transactions of the Asme*, 1998, 120(4), 716-723.
26
27 11 Bakhshi-Jooybari, M. A theoretical and experimental study of friction in metal
28 forming by the use of the forward extrusion process. *Journal of materials processing*
29 *technology*, 2002, 125-126, 369-374.
30
31 12 Flitta, I. and Sheppard, T. Nature of friction in extrusion process and its effect on
32 material flow. *Materials Science and Technology*, 2003, 19(7), 837-846.
33
34 13 Mori, T., Takatsuji, N., Matsuki, K., Aida, T., Murotani, K. and Uetoko, K.
35 Measurement of pressure distribution on die surface and deformation of extrusion die in
36 hot extrusion of 1050 aluminum rod. *Journal of materials processing technology*, 2002,
37 130-131, 421-425.
38
39 14 Abtahi, S. Interface mechanisms on the bearing surface in extrusion. *Sixth*
40 *International Aluminium Extrusion*, pp. 125-131 (Michigan, USA, 1996).
41
42 15 Tverlid, S. Modelling of friction in the bearing channel of dies for extrusion of
43 aluminium sections. 1997, PhD thesis.
44
45 16 Welo, T.A., S.; Skauvik, I.; Støren, S.; Melander, M.; Tjøtta, S. Friction in the
46 bearing channel of aluminium extrusion dies. *15th Riso International Symposium on*
47 *Materials Science*, pp. 615-620 (Roskilde, Denmark 1994).
48
49 17 Wang, L.-l., Zhou, J. and Duszczyk, J. Friction in double action extrusion. *Key*
50 *Engineering Materials*, 2010, 424, 153-160.
51
52
53
54
55
56
57
58
59
60
61
62
63
64
65

- 1
2
3
4 18 Wang, L., He, Y., Zhang, Y., Cai, J., Zhou, J., Duszczyc, J. and Katgerman, L.
5 Modeling of double action extrusion - a novel extrusion process for friction
6 characterization at the billet-die bearing interface. *Tribology International*, 2010, In press.
7
8
9 19 Olsson, M., Soderberg, S., Jacobson, S. and Hogmark, S. Simulation of cutting-
10 tool wear by a modified pin-on-disc test. *International Journal of Machine Tools &*
11 *Manufacture*, 1989, 29(3), 377-390.
12
13
14 20 Rech, J., Claudin, C. and D'Eramo, E. Identification of a friction model--
15 Application to the context of dry cutting of an AISI 1045 annealed steel with a TiN-
16 coated carbide tool. *Tribology International*, 2009, 42(5), 738-744.
17
18
19 21 Bonnet, C., Valiorgue, F., Rech, J., Claudin, C., Hamdi, H., Bergheau, J.M. and
20 Gilles, P. Identification of a friction model--Application to the context of dry cutting of
21 an AISI 316L austenitic stainless steel with a TiN coated carbide tool. *International*
22 *Journal of Machine Tools and Manufacture*, 2008, 48(11), 1211-1223.
23
24
25 22 Zemzemi, F., Rech, J., Ben Salem, W., Dogui, A. and Kapsa, P. Identification of a
26 friction model at tool/chip/workpiece interfaces in dry machining of AISI4142 treated
27 steels. *Journal of materials processing technology*, 2009, 209(8), 3978-3990.
28
29
30 23 Ranganatha, S., Kailas, S.V., Storen, S. and Srivatsan, T.S. Role of temperature
31 on sliding response of aluminum on steel of a hot extrusion. *Materials and Manufacturing*
32 *Processes*, 2008, 23(1), 29-36.
33
34
35 24 Wang, L.L., Cai, J.Q., Zhou, J. and Duszczyc, J. Characteristics of the Friction
36 Between Aluminium and Steel at Elevated Temperatures During Ball-on-Disc Tests.
37 *Tribology Letters*, 2009, 36(2), 183-190.
38
39
40 25 Bay, N., Olsson, D.D. and Andreasen, J.L. Lubricant test methods for sheet metal
41 forming. *Tribology International*, 2008, 41(9-10), 844-853.
42
43
44 26 Tan, X.C., Bay, N. and Zhang, W.Q. On parameters affecting metal flow and
45 friction in the double cup extrusion test. *Scandinavian Journal of Metallurgy*, 1998, 27(6),
46 246-252.
47
48
49 27 Schrader, T., Shirgaokar, M. and Altan, T. A critical evaluation of the double cup
50 extrusion test for selection of cold forging lubricants. *Journal of materials processing*
51 *technology*, 2007, 189(1-3), 36-44.
52
53
54 28 Shirzadi, A.A., Assadi, H. and Wallach, E.R. Interface evolution and bond
55 strength when diffusion bonding materials with stable oxide films. *Surface and Interface*
56 *Analysis*, 2001, 31(7), 609-618.
57
58
59 29 Jiang, J., Arnell, R.D. and Dixit, G. The influence of ball size on tribological
60 behaviour of MoS₂ coating tested on a ball-on-disk wear rig. *Wear*, 2000, 243(1-2), 1-5.
61
62
63
64
65

- 1
2
3
4 30 Hegadekatte, V., Huber, N. and Kraft, O. Modeling and simulation of wear in a
5 pin on disc tribometer. Tribology Letters, 2006, 24(1), 51-60.
6
7
8 31 Schey, J.A. Tribology in metalworking : friction, lubrication, and wear.
9 (American Society for Metals, Metals Park, Ohio, 1983).
10
11 32 Wang, L., He, Y., Zhou, J. and Duszcyk, J. Modelling of plowing and shear
12 friction coefficients during high-temperature ball-on-disc tests. Tribology International,
13 2009, 42(1), 15-22.
14
15
16 33 Bhushan, B. Introduction to tribology. (John Wiley & Sons, New York, 2002).
17
18 34 Hutchings, I.M. Tribology : friction and wear of engineering materials. (CRC
19 Press, Boca Raton, 1992).
20
21 35 Bowden, F.P. and Tabor, D. The friction and lubrication of solids. (Clarendon
22 Press, Oxford,, 1950).
23
24
25 36 Björk, T., Westergård, R., Hogmark, S., Bergström, J. and Hedenqvist, P.
26 Physical vapour deposition duplex coatings for aluminium extrusion dies. Wear, 1999,
27 225-229(Part 2), 1123-1130.
28
29
30 37 Kong, T.F., Chan, L.C. and Lee, T.C. Experimental Study of Effects of Process
31 Parameters in Forge-Welding Bimetallic Materials: AISI 316L Stainless Steel and 6063
32 Aluminium Alloy. Strain, 2009, 45(4), 373-379.
33
34
35 38 Kong, T.F., Chan, L.C. and Lee, T.C. Weld Diffusion Analysis of Forming
36 Bimetallic Components Using Statistical Experimental Methods. Materials and
37 Manufacturing Processes, 2009, 24(4), 422-430.
38
39
40 39 Sahin, M. Joining of stainless-steel and aluminium materials by friction welding.
41 International Journal of Advanced Manufacturing Technology, 2009, 41(5-6), 487-497.
42
43 40 Ghosh, M., Bhanumurthy, K., Kale, G.B., Krishnan, J. and Chatterjee, S.
44 Diffusion bonding of titanium to 304 stainless steel. Journal of Nuclear Materials, 2003,
45 322(2-3), 235-241.
46
47
48 41 Moufki, A., Molinari, A. and Dudzinski, D. Modelling of orthogonal cutting with
49 a temperature dependent friction law. Journal of the Mechanics and Physics of Solids,
50 1998, 46(10), 2103-2138.
51
52 42 Wang, L., He, Y., Zhang, Y., Cai, J., Zhou, J., Duszcyk, J. and Katgerman, L.
53 Modeling of double action extrusion-A novel extrusion process for friction
54 characterization at the billet-die bearing interface. Tribology International, 2010, 43(11),
55 2084-2091.
56
57
58 43 Pluijms, G.J. Flow Stress Characterization of Aluminum Alloys in Warm and Hot
59 Working Conditions. (Delft University of Technology, Delft, 2008).
60
61
62
63
64
65

1
2
3
4
5
6
7
8
9
10
11
12
13
14
15
16
17
18
19
20
21
22
23
24
25
26
27
28
29
30
31
32
33
34
35
36
37
38
39
40
41
42
43
44
45
46
47
48
49
50
51
52
53
54
55
56
57
58
59
60
61
62
63
64
65

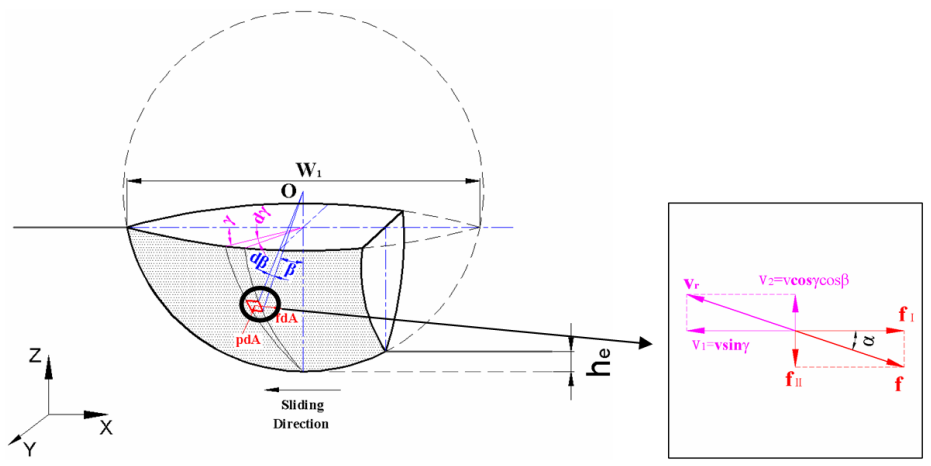


Figure 1 Close-up view of the friction force and velocity on an elemental area

1
2
3
4
5
6
7
8
9
10
11
12
13
14
15
16
17
18
19
20
21
22
23
24
25
26
27
28
29
30
31
32
33
34
35
36
37
38
39
40
41
42
43
44
45
46
47
48
49
50
51
52
53
54
55
56
57
58
59
60
61
62
63
64
65

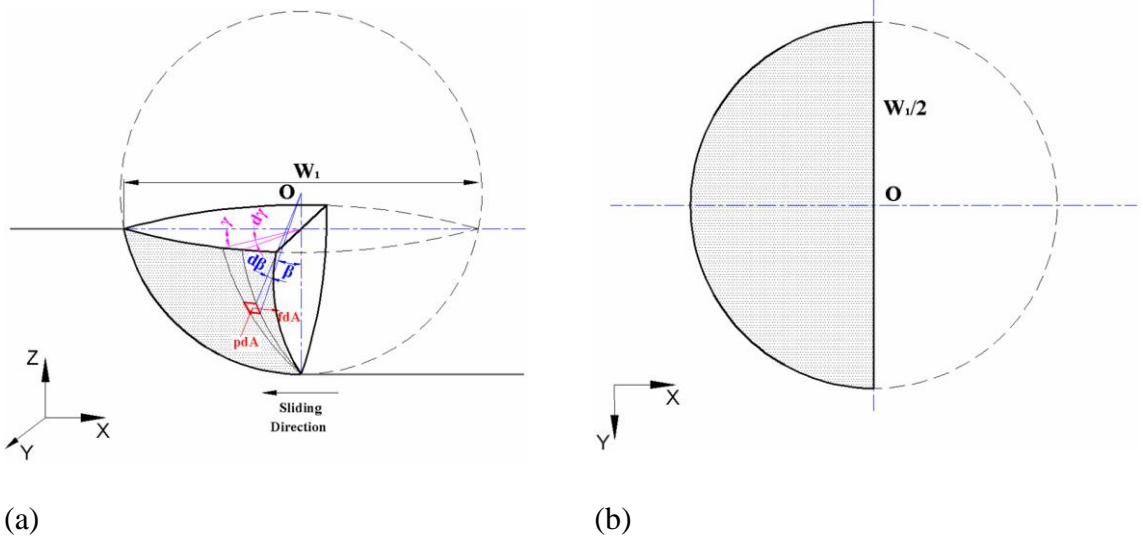


Figure 2 Schematic drawing of the contact interface in the first lap of wear during ball-on-disc testing

1
2
3
4
5
6
7
8
9
10
11
12
13
14
15
16
17
18
19
20
21
22
23
24
25
26
27
28
29
30
31
32
33
34
35
36
37
38
39
40
41
42
43
44
45
46
47
48
49
50
51
52
53
54
55
56
57
58
59
60
61
62
63
64
65

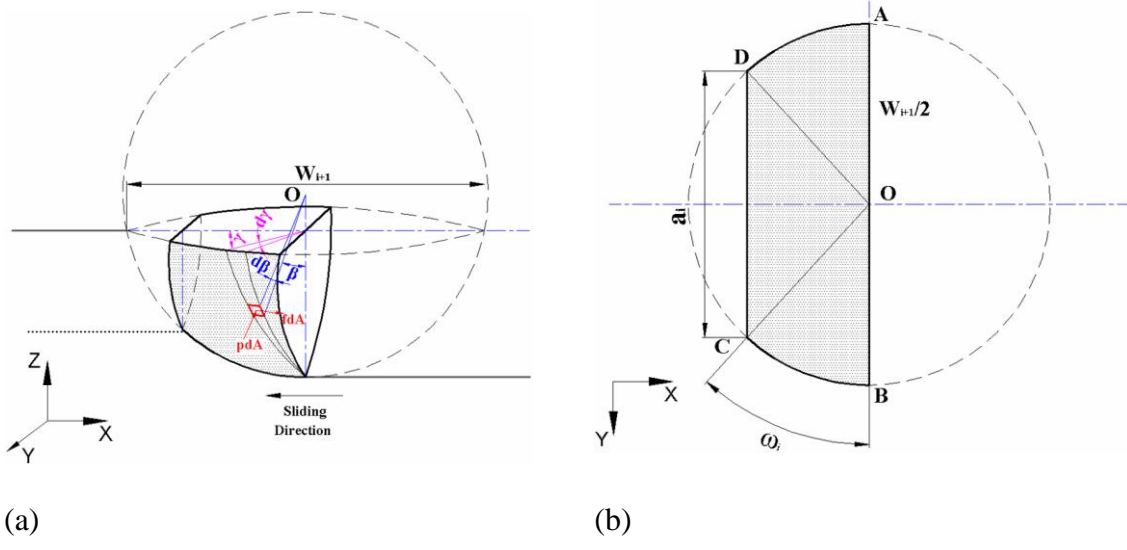


Figure 3 Schematic drawing of the contact interface in an arbitrary $(i+1)th$ lap of wear during ball-on-disc testing

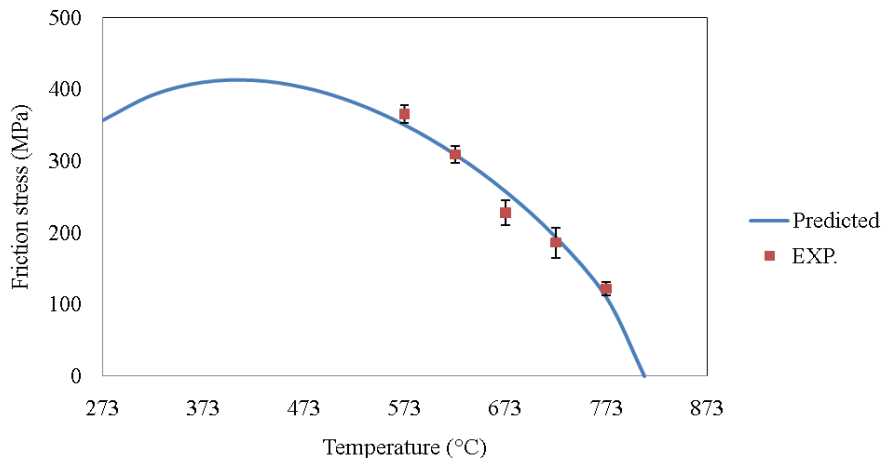


Figure 4 Evolution of friction stress between AA7475 and H11 steel at different temperatures

1
2
3
4
5
6
7
8
9
10
11
12
13
14
15
16
17
18
19
20
21
22
23
24
25
26
27
28
29
30
31
32
33
34
35
36
37
38
39
40
41
42
43
44
45
46
47
48
49
50
51
52
53
54
55
56
57
58
59
60
61
62
63
64
65

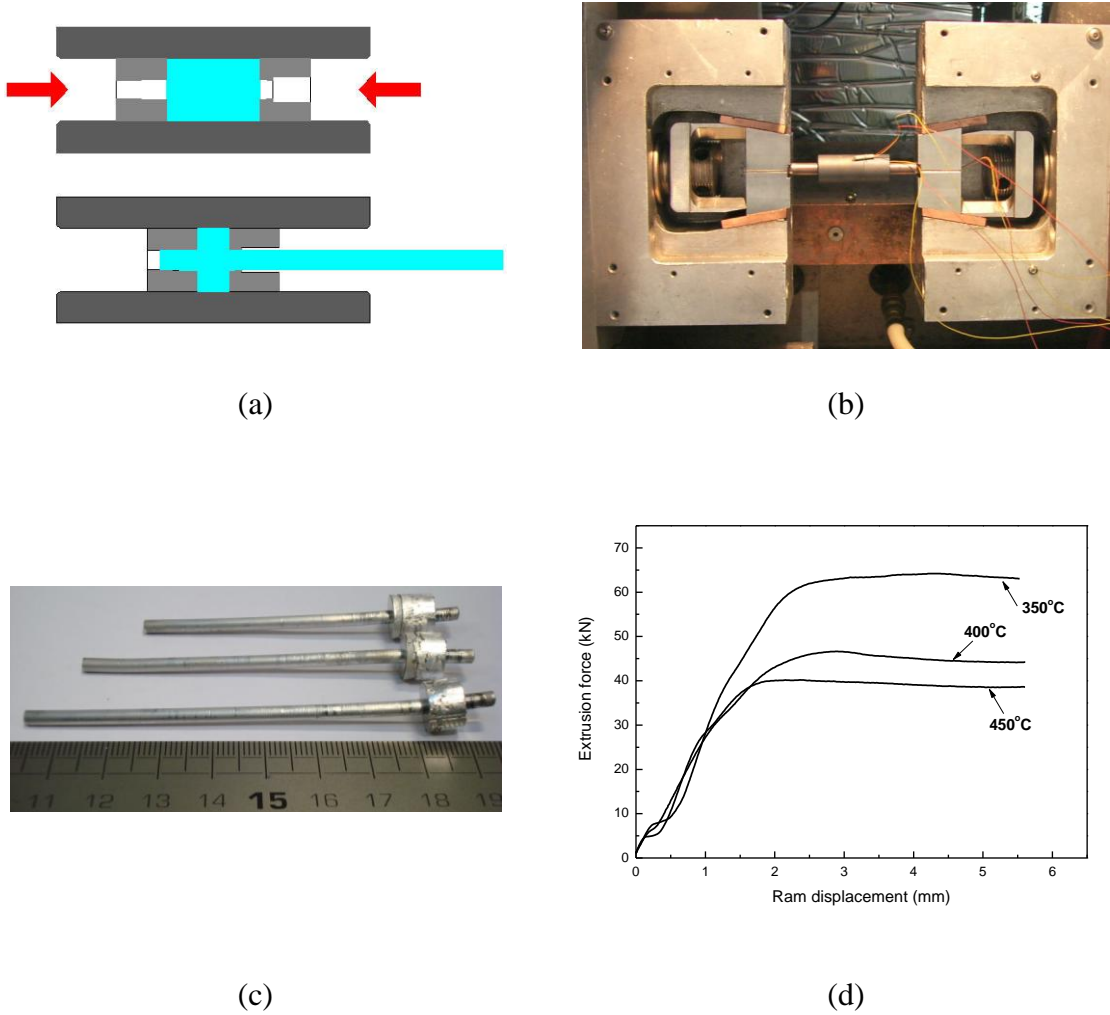


Figure 5 The (a) principle, (b) experimental setup and (c and d) typical test results of DAE

1
2
3
4
5
6
7
8
9
10
11
12
13
14
15
16
17
18
19
20
21
22
23
24
25
26
27
28
29
30
31
32
33
34
35
36
37
38
39
40
41
42
43
44
45
46
47
48
49
50
51
52
53
54
55
56
57
58
59
60
61
62
63
64
65

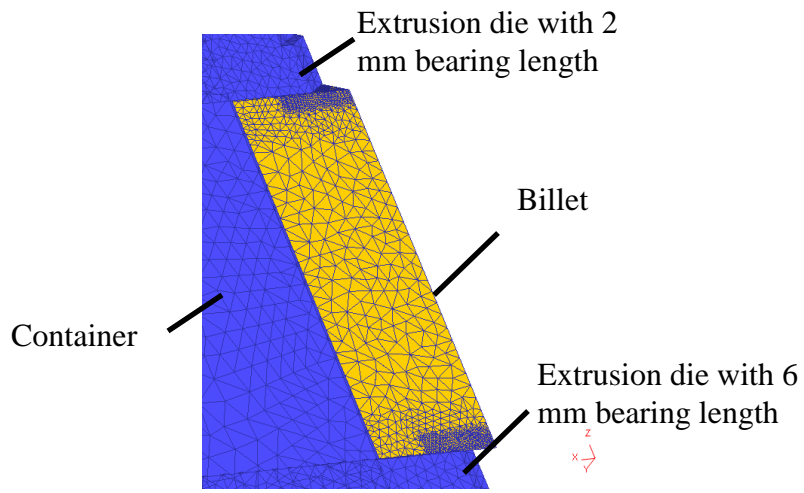


Figure 6 FE model for the DAE

1
2
3
4
5
6
7
8
9
10
11
12
13
14
15
16
17
18
19
20
21
22
23
24
25
26
27
28
29
30
31
32
33
34
35
36
37
38
39
40
41
42
43
44
45
46
47
48
49
50
51
52
53
54
55
56
57
58
59
60
61
62
63
64
65

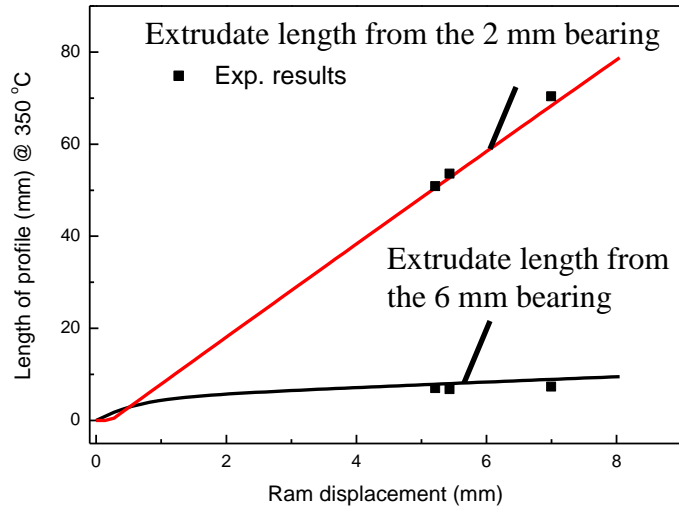


Figure 7 Comparison in the extrudate lengths from DAE at 350°C between the experiments and FEM simulations.

1
2
3
4
5
6
7
8
9
10
11
12
13
14
15
16
17
18
19
20
21
22
23
24
25
26
27
28
29
30
31
32
33
34
35
36
37
38
39
40
41
42
43
44
45
46
47
48
49
50
51
52
53
54
55
56
57
58
59
60
61
62
63
64
65

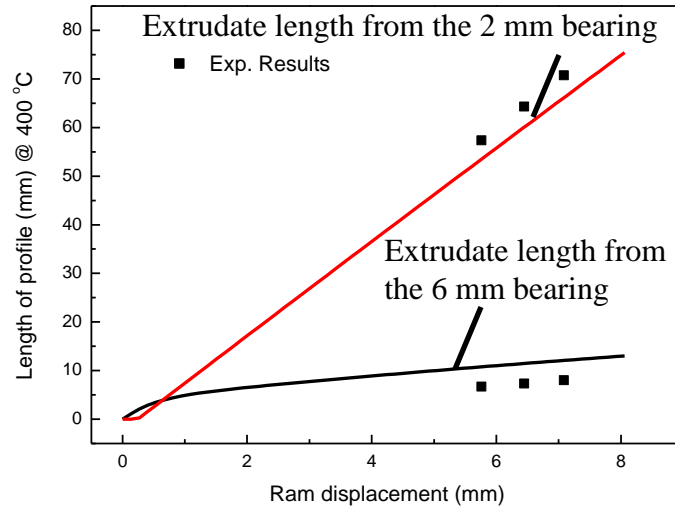


Figure 8 Comparison in the extrudate lengths from DAE at 400°C between the experiments and FEM simulations.

1
2
3
4
5
6
7
8
9
10
11
12
13
14
15
16
17
18
19
20
21
22
23
24
25
26
27
28
29
30
31
32
33
34
35
36
37
38
39
40
41
42
43
44
45
46
47
48
49
50
51
52
53
54
55
56
57
58
59
60
61
62
63
64
65

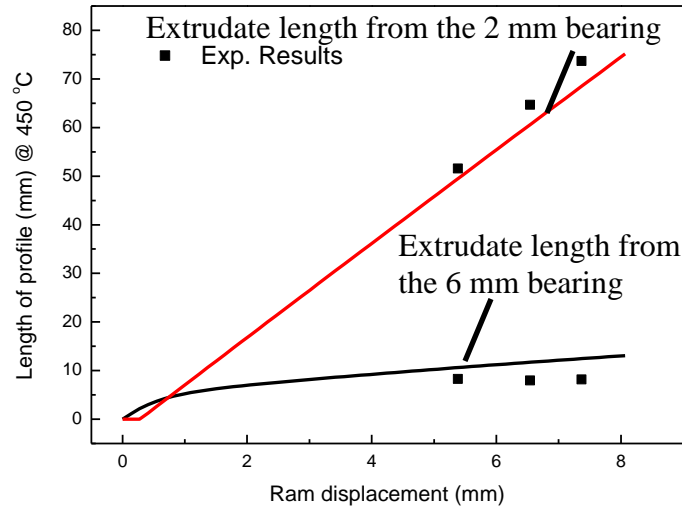


Figure 9 Comparison in the extrudate lengths from DAE at 450°C between the experiments and FEM simulations.

1
2
3
4
5
6
7
8
9
10
11
12
13
14
15
16
17
18
19
20
21
22
23
24
25
26
27
28
29
30
31
32
33
34
35
36
37
38
39
40
41
42
43
44
45
46
47
48
49
50
51
52
53
54
55
56
57
58
59
60
61
62
63
64
65

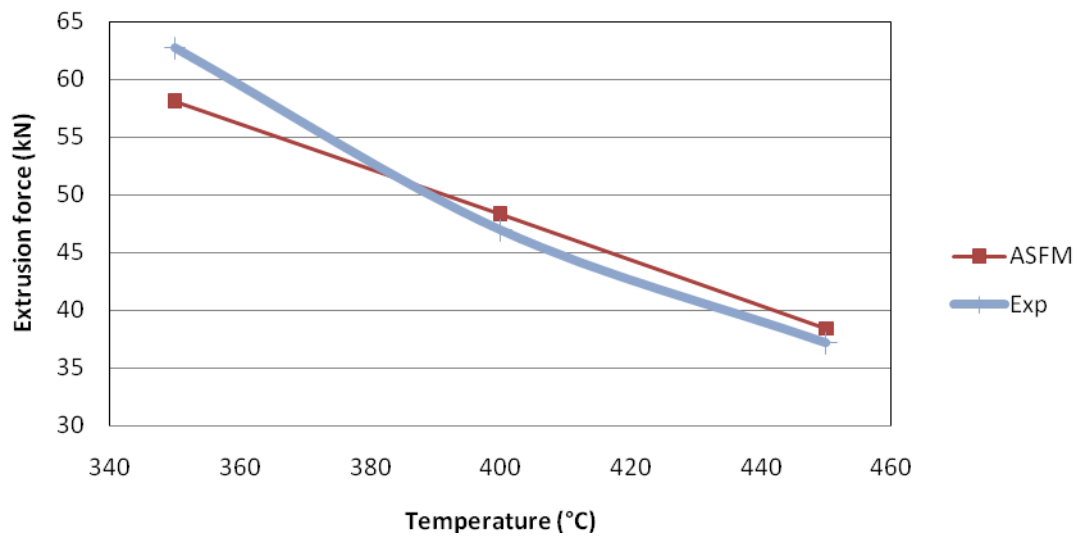


Figure 10 Steady state extrusion forces at different extrusion temperatures

1
2
3
4 **Identification of a friction model for the bearing channel of hot**
5
6
7 **aluminium extrusion dies by using ball-on-disc tests**
8
9

10
11
12 Liliang Wang*, Jie Zhou, Jurek Duszczuk and Laurens Katgerman
13
14

15
16
17 *Department of Materials Science and Engineering, Delft University of Technology,*
18
19
20 *Mekelweg 2, 2628 CD Delft, The Netherlands*
21
22

23
24
25 **Abstract**
26

27
28
29
30 A physically-based friction model is developed based on the ball-on-disc test results. The
31
32 model is verified by using double action extrusion tests. Good agreements between the
33
34 FE predictions and experiments have been obtained, in terms of the extrudate length and
35
36 steady-state extrusion load, indicating that ball-on-disc test is an effect way of
37
38 characterizing the friction for the bearing channel of hot extrusion dies. The nature of
39
40 friction in the bearing channel can be summarized as a pressure dependant process:
41
42 formation of isolated adhesive junctions, adhesive junctions growth and coalescence of
43
44 adhesive junctions.
45
46
47
48
49
50

51
52 *Keywords:* FE Simulation; Friction model; Hot aluminium extrusion; Bearing channel
53
54
55

56 * Corresponding author.
57

58
59 E-mail address: Liliang.wang@gmail.com
60
61

1
2
3
4
5
6
7
8
9 **1. Introduction**

10
11
12
13
14 Extrusion is a process in which a cast billet of solid metal is converted into a continuous
15
16 length of generally uniform cross-section by forcing it to flow through a shaped die
17
18 opening. Generally, the extrusion process is a hot working operation, in which the metal
19
20 billet is heated to a proper temperature, at which a relatively high ductility and low flow
21
22 stress can be achieved. FE simulation of the extrusion processes is widely used in both
23
24 scientific research and industrial practice. The selection of friction models and the
25
26 assignment of friction coefficients or factors for the FE simulations of extrusion
27
28 processes remain an essential issue, because the accuracy of the simulation results is
29
30 strongly affected by the flow stress of workpiece material (thermo-viscoplastic behavior
31
32 at elevated temperatures) and the assignment of boundary conditions, *e.g.* friction
33
34 boundary conditions. The uncertainty of flow stress is low when the constitutive
35
36 equations determined from thermo-mechanical testing are implemented. However,
37
38 unreliable FE simulation results could be obtained if the friction boundary conditions are
39
40 not assigned appropriately.
41
42
43
44
45
46
47
48
49

50
51 In the past years, efforts have been made to study the tribological phenomenon of the
52
53 extrusion process and some friction testing techniques have been developed, which can
54
55 be classified as three different categories, namely, field tests; simulative tests (or physical
56
57 simulation tests) and tribological tests.
58
59
60
61

1
2
3
4
5
6
7 In general, field test is to estimate the friction coefficient or factor by using extrusion
8
9 friction tests. Based on the material flow response to the friction force, some novel
10
11 extrusion friction tests have been developed, including double backward extrusion [1],
12
13 combined forward rod-backward can extrusion [2] and combined forward conical /
14
15 straight can-backward straight can extrusion [3]. These tests were designed with
16
17 highlighted friction sensitivity indicated by extrudate lengths, and the lubricants can be
18
19 evaluated and the global friction coefficient or factor on the workpiece/tooling interface
20
21 can be determined quantitatively with the aid of FE simulations. On the other hand, the
22
23 friction coefficients/factors over the container wall can be estimated based on the friction
24
25 effects on the extrusion load [4, 5]. Table 1 shows a summary of the friction test results
26
27 obtained from extrusion friction tests. For the friction at extrudate/bearing interface,
28
29 extrusion friction test [6-8] was used to characterize the friction in this region. A
30
31 transition from full sticking to sliding was experimentally observed and the friction stress
32
33 was therefore determined from the lengths of sticking and sliding zones [6, 7, 9].
34
35
36
37
38
39
40
41
42
43
44
45
46
47
48
49
50
51
52
53
54
55
56
57
58
59
60
61
62
63
64
65

Table 1 friction test results obtained from extrusion friction tests

Extrusion test	Work piece material	Tool material	Billet temp. (°C)	Die temp. (°C)	Lub(s)	Friction coef./factor
1992 Buschhausen <i>et al.</i> [1]	AISI 1006		25	25	Lub	m=0.08-0.2
1997 Nakamura <i>et al.</i> [2]	6061	High speed steel	-	-	Ca-Al	$\mu \approx 0.3-0.4$
					VG26	$\mu \approx 0.5$
					MoS ₂	$\mu \approx 0.5-0.6$
1998 Nakamura <i>et al.</i> [3]	6061	High speed steel, cemented carbide	-	-	VG2	$\mu_d = 0.017-0.05$ $\mu_{LP} = 0.37-0.42$
					VG26	$\mu_d = 0.005-0.048$ $\mu_{LP} = 0.15-0.19$
					VG1000	$\mu_d = 0.001-0.039$ $\mu_{LP} = 0.15-0.28$
					MoS ₂	$\mu_d = 0.088-0.105$ $\mu_{LP} = 0.07-0.18$
2002 Bakhshi-Jooybari [4]	CP Al	H13	25	25	No Lub.	m=0.84
	Steel		900	900	Graphite	-
2003 Flitta <i>et al.</i> [5]	AA2024 Al-Cu ally	-	300-450	250-400	No Lub.	m=0.654-0.92

Field tests are normally time consuming, expensive and difficult to control. In most of the field tests, the local contact conditions vary significantly throughout the whole operating cycle. Therefore, there is a need for simplified friction testing techniques, in which more stable contact conditions can be achieved. As such, simulative friction tests have been proposed and conducted. The block on cylinder tests [10, 11] were developed to simulate the contact between the workpiece and extrusion die, and the wear mechanisms in the bearing channel region were studied. The results revealed that adhesive wear and

1
2
3
4 abrasive wear were dominant wear patterns of the extrusion dies. In the meanwhile, high
5
6 values of friction coefficients ($1 < \mu < 1.5$) were observed and this was attributed to a high
7
8 degree of aluminium to aluminium contact [11]. Most recently, a novel simulative
9
10 friction test method highlighting the friction in the bearing channel of the die, double
11
12 action extrusion (DAE), was developed [12]. In the DAE, an aluminium billet was
13
14 pressed against two extrusion dies with different bearing lengths and two indirect
15
16 extrusions took place simultaneously. The lengths of the extrudates were found to be
17
18 highly friction sensitive, because the friction force for the extrudate to flow through the
19
20 die with a longer bearing length was greater than that through the die with a shorter
21
22 bearing length. As such, friction between the extrudate and bearing channel of the
23
24 extrusion dies can be characterized, with the aid of FE simulation [12] or theoretical
25
26 analysis [13]. The results obtained from the DAE tests indicate that full sticking friction
27
28 occurred at the extrudate/die interface when a 15' choke angle was applied in the
29
30 extrusion dies [12, 13].
31
32
33
34
35
36
37
38
39
40

41 In the field tests or simulative tests, it is difficult to study the effects of individual factor,
42
43 such as temperature, sliding speed or contact pressure *etc.*, on the friction. As such,
44
45 tribological test is probably a sensible technique to reveal the mechanisms of friction
46
47 under hot aluminium extrusion conditions. Tribological tests (pin/ball-on-disc tests) have
48
49 been employed previously to identify the friction coefficients for metal cutting process
50
51 [14-17]. Recently, the first attempt has been made to simulate the interactions at bearing
52
53 surface by using ball/pin-on-disc tests [18]. The steady-state friction was found to be
54
55 greater than 1.0 when the testing temperature was higher than 150°C and the magnitude
56
57
58
59
60
61
62
63
64
65

1
2
3
4 of friction increased with increasing temperature. The presence of a continuous transfer
5
6 layer was thought to be responsible for the high magnitude of the frictional force.
7
8
9

10
11 Although more efforts have been made previously to simulate the extrudate/bearing
12 interactions by using tribological tests [19, 20], the fundamental understanding of the
13 friction phenomenon in the bearing channel of hot aluminium extrusion dies is still
14 insufficient, and the tribological test results have not been implemented into the FE
15 simulations of hot aluminium extrusion yet. The aim of this research is to understand the
16 fundamental of friction phenomenon in the bearing channel of hot extrusion die from a
17 tribological point of view. Moreover, based on the ball-on-disc test results, a physically-
18 based friction model has been developed and implemented into the simulation of hot
19 aluminium extrusion process.
20
21
22
23
24
25
26
27
28
29
30
31
32
33
34
35

36 **2. Selection of friction testing techniques for the friction characterization of hot** 37 **aluminium extrusion processes** 38 39 40 41 42

43 During a friction test, the large variety of contact conditions, such as temperature, contact
44 pressure, sliding distance, sliding velocity and oxidation scale should be considered very
45 carefully [21], because these factors may influence the friction coefficients considerably.
46
47 In general, it is very unlikely to emulate all the contact conditions or reflect all the
48 tribological conditions by using one single friction testing technique, because one friction
49 testing technique is only able to reflect one specific or a few tribological conditions, *i.e.*
50 the tribological conditions of a particular region of the workpiece / tooling interface.
51
52 Therefore, for the friction characterization of extrusion processes, a combination of
53
54
55
56
57
58
59
60
61
62
63
64
65

1
2
3
4 different testing methods should be used, for instance, the combination of extrusion
5
6 friction tests (to determine the friction at billet / container interface) and short sliding
7
8 distance ball-on-disc tests (to determine the friction in the bearing channel region).
9

10
11
12
13
14 Extrusion friction tests were developed to estimate the global friction coefficient at the
15
16 billet/container interface. During the tests, high contact pressure and intensive surface
17
18 enlargement can be achieved [2, 3, 5, 22, 23]. Most recent research results have shown
19
20 that different contact conditions in the extrusion friction tests can be achieved by
21
22 adjusting the extrusion ratio[23]: low contact pressure and surface enlargement can be
23
24 achieved when low extrusion ratio is used, thus high level of friction sensitivity can be
25
26 achieved. If a high extrusion ratio is used, high contact pressure and surface enlargement
27
28 are obtained, which resemble the real contact condition of forging or extrusion processes,
29
30 but sacrifice the friction sensitivity. The combination of extrusion friction tests and FEM
31
32 simulations is an effective way to estimate global friction at the billet and container
33
34 interface.
35
36
37
38
39
40
41
42

43 Ball/pin-on-disc test is a widely used laboratory testing technique for the quantitative
44
45 study of tribological behavior of materials. During ball-on-disc tests, high contact
46
47 pressure can be achieved in a small contact area between the ball and the rotating disc. If
48
49 a soft material is sliding over a harder one, severe plastic deformation may occur in the
50
51 soft material, which could lead to the removal of oxide layers and the contact of pure
52
53 metals. In the meanwhile, the contact pressure may drop with the increasing sliding
54
55 distance. Therefore, ball-on-disc tests are favorable to the friction characterization of the
56
57
58
59
60
61
62
63
64
65

1
2
3
4 regions, in which local contact pressure is high and new surface generation is severe,
5
6 such as the bearing channel of hot aluminium extrusion dies. During hot aluminium
7
8 extrusion, fresh aluminium is extruded from the container, and in the die bearing, a pure
9
10 metal contact takes place. It is well known that the presence of chemical stable surface
11
12 oxides or scale prevents the strong atomic interactions [24]. Therefore, in order to
13
14 reproduce the friction conditions in the bearing channel, it is vital to choose a friction
15
16 testing technique being able to remove the surface oxides. Short sliding distance ball-on-
17
18 disc test is one of the best friction testing techniques over the other ones, because during
19
20 the ball-on-disc tests, severe plastic deformation occurs at the ball / disc interface [14, 15,
21
22 18], especially during the run-in period. Therefore, it is highly suitable for the study of
23
24 friction between fresh metals, which emulates the contact condition in the bearing
25
26 channel or welding chamber of the extrusion dies. However, the friction test results
27
28 obtained from ball-on-disc tests cannot be translated into friction boundary conditions for
29
30 the FE simulations of extrusion processes directly. Therefore, the selection of testing
31
32 parameters, such as pin and disc materials, sliding distance and size of the ball has to be
33
34 considered carefully. Furthermore, friction data processing has to be conducted with the
35
36 aid of FEM simulation or theoretical analysis.
37
38
39
40
41
42
43
44
45
46
47

48 The selection of the pin and disc materials affects ball-on-disc test results. If the pin is
49
50 made from a soft material, and the disc is made from a hard one, severe plastic
51
52 deformation and wear would occur on the tip of the pin, which leads to a significant
53
54 enlargement of the contact area. After the run-in period, a steep decrease of contact
55
56 pressure occurs and the contact pressure during the steady-state sliding is close to or
57
58
59
60
61
62
63
64
65

1
2
3
4 lower than the yield strength of the soft material. On the other hand, if the disc is made
5
6 from a soft material, while the pin is made from a hard one, plastic deformation tends to
7
8 occur in the disc, but the material flow is most likely constrained by the remainder disc
9
10 material, which is much larger than the size of the wear track. Hence a relatively high
11
12 hydrostatic pressure which is greater than the strength of the disc material could be
13
14 imposed onto the spherical pin head. Therefore, different materials combinations would
15
16 result in different contact pressures, and the selection of pin and disc mating materials
17
18 need to be considered carefully prior to testing, especially when the strengths of the pin
19
20 and disc materials are different. In the meanwhile, the selection of ball size and sliding
21
22 distance is of great importance. In general, the contact pressure decreases with increasing
23
24 ball size [25] and increasing sliding distance [26].
25
26
27
28
29
30
31
32

33 When a hard pin is sliding over a soft disc, the apparent friction coefficient obtained from
34
35 the test is normally composed of plowing and shearing (adhesive) friction [15, 16, 27].
36
37 The plowing friction is caused by the plastic deformation of the disc material in front of
38
39 the pin, which depends on the size of the ball, sliding distance and the material strength.
40
41 Consequently, the test results cannot be transferred into a metal forming operation
42
43 directly, because the existence of plowing friction leads to an overestimation of the
44
45 friction between the mating materials. The plowing and shear friction have to be
46
47 discriminated by means of FEM simulations [15, 16] or theoretical analysis [19, 28], and
48
49 only the shear component of apparent friction representing the real friction between the
50
51 two mating materials should be used in the FE simulations of metal forming operations as
52
53 boundary conditions [15, 16]. However, when the material combination of soft pin and
54
55
56
57
58
59
60
61
62
63
64
65

1
2
3
4 hard disc is used, the friction coefficients obtained from the tests are mainly attributed to
5
6 the shearing (adhesive) friction. Therefore, with the knowledge of contact pressure
7
8 evolution, the results can be transferred into the FE simulations as friction boundary
9
10 conditions. To simulate the tribological conditions in the bearing channel of the hot
11
12 aluminium extrusion die, short sliding distance ball-on-disc test is recommended, with
13
14 the disc made from the workpiece material and ball made from the die material.
15
16
17
18
19
20

21 **3. Determination of friction coefficient for the bearing channel of hot** 22 **aluminium extrusion dies by using ball-on-disc tests** 23 24 25 26 27

28 A CSM® high-temperature tribometer with a ball-on-disc configuration was used for the
29
30 friction characterization. To emulate the extrusion process, the disc was made from
31
32 AA7475 aluminium alloy, which was the same as the billet material used in the extrusion
33
34 tests. The hardened H11 steel was selected as the mating material, which was the same
35
36 material as that of extrusion dies. The tests were carried out under a constant normal load
37
38 of 6 N at 350, 400, 450 and 500°C [19]. In order to achieve a high contact pressure
39
40 between the mating materials, short sliding distance (1, 5 and 10 laps of sliding) ball-on-
41
42 disc tests were employed to represent the friction condition in the bearing channel of hot
43
44 aluminium extrusion process. Figure 1 shows the evolution of the friction coefficient over
45
46 a sliding distance of 10 laps at different temperatures. It is of interest to note that friction
47
48 coefficient increases with the sliding distance. At 500 °C, in particular, the friction
49
50 coefficient increases even by 50%. The increase of the friction coefficient with sliding
51
52 distance, leads to the uncertainty as to the exact value to be put into FE simulation. It is
53
54 therefore necessary to have a model with which the friction coefficient and sliding
55
56
57
58
59
60
61
62
63
64
65

distance are correlated with each other. A previously developed model being able to characterize the evolution of contact interface during high-temperature ball-on-disc tests was used to determine the mean friction stresses at different temperatures [19]. The details of this model is shown below:

Figure 2 shows the forces acting on an elemental area during ball-on-disc testing, which are given in Equation (1).

$$\begin{cases} dF_x = \left(pr^2 \sin^2 \beta \cos \gamma + fr^2 \sin \beta \sqrt{\cos^2 \gamma \cos^2 \beta + \sin^2 \gamma} \right) d\gamma d\beta \\ dF_z = \left(pr^2 \cos \beta \sin \beta - fr^2 \frac{\cos \gamma \sin^2 \beta \cos \beta}{\sqrt{\cos^2 \gamma \cos^2 \beta + \sin^2 \gamma}} \right) d\gamma d\beta \end{cases} \quad (1)$$

First lap of wear

The aluminium disc was assumed to behave as a viscoplastic material at elevated temperatures and the elastic recovery of the disc at the rare part of the ball was omitted. Figure 3 schematically shows the contact interface during the 1st lap of wear. Equation (2) can be used to calculate the tangential and normal forces acting on the ball surface.

$$\begin{cases} F_x = 2 \int_0^{\xi_1} \int_0^{\pi/2} dF_x \\ F_z = 2 \int_0^{\xi_1} \int_0^{\pi/2} dF_z \end{cases} \quad (2)$$

where ξ_1 is the upper integral limit of angle β (see Figure 3a where W_1 is the width of the wear track after the first lap of wear).

1
2
3
4 *Arbitrary (i+1)th lap of wear*
5
6

7 The contact interface of an arbitrary lap of wear is schematically shown in Figure 4. The
8 tangential and normal forces acting on the ball can be calculated by Equation (3).
9
10

$$\begin{cases} F_x = 2 \int_0^{f_i(\gamma)} \int_0^{\pi/2-\omega_i} dF_x + 2 \int_0^{\xi_i} \int_{\pi/2-\omega_i}^{\pi/2} dF_x \\ F_z = 2 \int_0^{f_i(\gamma)} \int_0^{\pi/2-\omega_i} dF_z + 2 \int_0^{\xi_i} \int_{\pi/2-\omega_i}^{\pi/2} dF_z \end{cases} \quad (3)$$

11
12
13
14
15
16
17
18
19
20
21

22 As shown in Figure 4b, in the area *COD*, $f_i(\gamma)$ is the upper integral limit of β , and in
23 the areas *AOD* and *COB*, ξ_i is the upper integral limit of angle β . ω_i is the angle for
24 locating the position of the front contact boundary during the $(i+1)th$ lap of wear. The
25 shear friction stresses at different temperatures were determined by using Equations 1-3.
26
27 Figure 5 shows the evolutions of the calculated shear friction stress at different
28 temperatures and over a sliding distance of 10 laps. It is interesting to see that the shear
29 friction stress starts from a relatively low value, and then becomes stable at different
30 temperatures, while the friction coefficient increases considerably (Figure 1). The low
31 shear friction stress at the initial stage may be due to the oxide layer on the disc and ball
32 surfaces, which tends to lower the adhesion between aluminium and steel [29, 30]. After
33 the initial stage of sliding, the oxide layer may be broken up and metal-to-metal contact
34 occurs, leading to the increases in friction stress. In addition, the severe plastic
35 deformation on the surface material may generate a considerable work-hardening effect
36 [31, 32], which may also lead to the rise of shear friction stress.
37
38
39
40
41
42
43
44
45
46
47
48
49
50
51
52
53
54
55
56
57
58
59
60
61
62
63
64
65

1
2
3
4 **4. A physically-based adhesive strength friction model (ASFM) for the bearing**
5 **channel of hot aluminium extrusion die**
6
7
8
9

10
11 According to the classic theory of tribology, the friction force mainly stems from
12 ploughing (due to hard asperities and trapped wear debris) and adhesive (due to atomic or
13 chemical interactions) forces [31-33]. At elevated temperatures, the adhesive friction
14 plays a dominant role, due to the strong atomic or chemical interactions. The adhesive
15 friction becomes more pronounced under high contact pressures [11, 34-36]. This is
16 mainly caused by the following reasons: at elevated temperatures, the atoms in both
17 materials in contact are highly active, which aids the interdiffusion at the surface layers
18 of the materials and a strong chemical bonding tends to be formed. The mating materials
19 and surface oxides are relatively soft and easy to be deformed or penetrated, which thus
20 leads to the contact of pure metals. In addition, the high contact pressure (several times
21 greater than the flow stress of the workpiece material) further aids the severe plastic
22 deformation of the asperities or oxidation scale, and brings the faying material highly
23 close to each other to a distance of atomic level. Therefore, in the bearing channel of hot
24 aluminum extrusion, the strong chemical or diffusion bonding is the dominant friction
25 mechanism, which has been verified experimentally before [11, 34-36]. Also, the strong
26 interactions between hot Al and steel have been observed in the forge welding process
27 [37-39]. From a micro-scale point of view, the influence of the contact pressure is to
28 change the real contact area, *i.e.* the number of asperities in contact. Therefore, the nature
29 of different friction modes within the bearing channel could be summarized as:
30
31
32
33
34
35
36
37
38
39
40
41
42
43
44
45
46
47
48
49
50
51
52
53
54
55
56
57
58
59

60 Formation of isolated adhesive junctions → Adhesive junctions growth → Coalescence
61
62
63
64
65

1
2
3
4 of adhesive junctions.
5
6
7

8
9 *Formation of isolated adhesive junctions.* At low contact pressure conditions, full
10 sticking occurs on the tips of plastically deformed asperities, but the faying surfaces are
11 only supported by a small number of asperities [40, 41], thus only a few isolated adhesive
12 junctions are formed and normally too small to be observed by the naked eye. At this
13 stage, no adhesive layers can be observed in the bearing channel of the extrusion dies.
14 Therefore a so-called slipping zone can be observed experimentally, as shown in Figure 6
15 (b) and (d) [11].
16
17
18
19
20
21
22
23
24
25
26
27

28 *Adhesive junctions growth.* As the increase of contact pressure, the number of plastically
29 deformed asperities is increased [40, 41], to support the increased contact pressure. In
30 some regions with a higher asperity density, adhesive junctions growth takes place due to
31 the plastic deformation and some of the adhesive junctions may coalesce to each other
32 locally to form contact patches [40, 41]. Consequently, some of the work piece material
33 or intermetallic wear debris may transfer from the extrudates to the bearing surface of the
34 die, due to the strong adhesive bonding [42-44]. It is worth noting that, during hot
35 aluminium extrusion, the temperature of the extrusion die is normally lower than that of
36 the billets, and thus the strength of the adhesive junctions is enhanced once they are
37 formed and adhere onto the extrusion die, as the temperature drops. Therefore, the size of
38 the adhesive junctions might “grow” bigger and bigger, with the aggregation of wear
39 debris, i.e. the “lump growth” occurs [42, 45], which might be one of the reasons for the
40 generation of extrusion surface defects, such as die line and pick-up. At this stage, an in-
41
42
43
44
45
46
47
48
49
50
51
52
53
54
55
56
57
58
59
60
61
62
63
64
65

1
2
3
4 continuous tribo-layer might be visible on the die land, and the so-called transition zone
5
6 between the slipping and sticking zone may be observed, as shown in Figure 6 (b) and (c)
7
8 [11]. According to [6], the transition zone is normally observed when extruding with low
9
10 die temperatures, and this region is composed of a sportlike aluminium deposit.
11
12
13
14

15
16 *Coalescence of adhesive junctions.* At the die entrance, where a high contact pressure is
17
18 achieved, the real contact area is maximized, thus the number of adhesive junctions is
19
20 significantly increased and they are close to each other, thus tend to coalesce with each
21
22 other. Moreover, a great amount of workpiece material may transfer from the extrudates
23
24 to the bearing surface of the die, due to the strong adhesive bonding. Therefore there
25
26 exists a great chance for the adhesive junctions within a large area to coalesce with each
27
28 other and thus the adhesive junctions can be observed by the naked eye. At this stage, a
29
30 continuous tribo-layer, *i.e.* the so-called adhesive zones, can be observed on the bearing
31
32 surface. However, after extrusion, the inlet of the bearing is heavily worn and a
33
34 continuous tribo-layer may not be observed, as shown in Figure 6 (a) and (b) [11]. This is
35
36 probably due to the high rate of material renewal at the inlet of the bearing channel [34].
37
38
39
40
41
42
43
44

45
46 In this research, the strong adhesive friction generated from pure metal contact is
47
48 modelled, and the strength of adhesive junctions is considered to be determined by two
49
50 factors, namely, the rate of atomic interaction and the strength of adhesive joints
51
52 (Equation 6). The interaction rate at atomic level increases with increasing temperature,
53
54 which can be modeled by using an Arrhenius type equation [46] (Equation 7). The
55
56 bonding strength decreases with increasing temperature, due to the decreasing strength of
57
58
59
60
61
62
63
64
65

1
2
3
4 adhesive joints with increasing temperatures, and the bonding strength drops to zero at
5
6 the melting temperature of AA7475 (Equation 6). The friction stresses obtained from
7
8 short sliding distance ball-on-disc tests shown in Figure 5, were used to determine the
9
10 constants of the model. Table 2 lists the determined material constants. As can be seen
11
12 from Figure 7, a good agreement between the model and experimental results was
13
14 obtained.
15
16
17
18
19
20
21

$$f(T) = f_0 D \left(1 - \frac{T}{T_m}\right)^\eta \quad (6)$$

$$D = D_0 \cdot \exp\left(-\frac{Q_D}{RT}\right) \quad (7)$$

22
23
24
25
26
27
28
29
30
31
32 where $f(T)$ is temperature dependant bonding strength or friction stress in a unit area;

33
34
35 f_0 is the mean adhesive strength at room temperature (300 K) in a unit area;

36
37
38 D is the inter-diffusion coefficient at elevated temperatures;

39
40
41 T is the mean contact temperature;

42
43
44 T_m is the melting temperature of the workpiece material;

45
46
47 Q_D is the activation energy;

48
49
50 R is the universal gas constant;

51
52
53 D_0 and η are constants;
54
55
56
57
58
59
60
61
62
63
64
65

Table 2 Material constants of the ASFM for hot AA7475 and H11 steel

$f_0(MPa)$	$T_m (K)$	$Q_D(J/mol)$	$R(J/K/mol)$	D_0	η
378	811	2400	8.314	3.62	0.7

In this model, the bonding strength is determined by the combined effects of atomic interaction and the strength of adhesive joints, with the assumption that pure metal contact is taking place. At high temperatures ($0.5T_m < T \leq T_m$), the bonding strength decreases with increasing temperature, because the decreased strength of adhesive joints plays a dominant role, although the atoms are highly active and atomic interactions are more intensive at elevated temperatures. Therefore a decreased adhesive strength with the increasing temperature can be observed, which is consistent with other research results [31, 47].

5. Verification of the friction model

5.1. Experiment and FE simulation details

The double action extrusion (DAE) tests [17, 18], highlighting the friction in the bearing channel of the extrusion dies, were used to verify the proposed friction model. Figure 8 (a) shows the principle of DAE, which was conducted on a Gleeble 3800 material thermo-mechanical simulator and Figure 8 (b) shows the experimental setup. In the DAE tests, a combination of 2 and 6 mm bearing dies with a choke angle of 15° was employed to maximize the effect of friction in the bearing channels [48]. It has been found that the DAE is highly sensitive to the friction in the bearing regions, in terms of extrudate

1
2
3
4 lengths and steady-state extrusion load. Figure 8 (c) shows the typical test results of DAE
5
6 and the length differences were caused by the different friction forces generated from the
7
8 two different extrusion dies, with different bearing lengths used. Figure 8 (d) shows the
9
10 typical extrusion forces of DAE tests at different testing temperatures. As can be seen
11
12 from Figure 8 (d), the extrusion forces decreased with increasing temperature, mainly due
13
14 to the decreased strength of the workpiece material with rising temperature. The
15
16 extrusion forces at these temperatures showed a similar trend, *i.e.* a small plateau at the
17
18 very early stage, followed by a sharp increase in extrusion force and then a gentle
19
20 decrease as the process proceeded further. The small plateau corresponds to the initiation
21
22 of extrusion toward both of the die (upsetting) and the sharp force increase corresponds to
23
24 breakthrough. In DAE, there is no friction between the billet and container and therefore
25
26 the extrusion force in the steady state reflects a dynamic balance between the deformation
27
28 force of the workpiece material and the friction forces in the two dies which are governed
29
30 by temperature.
31
32
33
34
35
36
37
38
39
40

41 DEFORM 3D version 6.1 was used to simulate the DAE process. Figure 9 shows the
42
43 FEM model of the DAE. All the objects in the model were meshed with tetrahedral
44
45 elements. The flow stress data of AA7475 aluminium alloy were determined from hot
46
47 compression tests on a Gleeble 3800 material thermomechanical simulator, under a wide
48
49 range of strain rate ($0.01-180 \text{ s}^{-1}$), with the data at high strain rates corrected for
50
51 deformational heating [49]. The ASFM were implemented into DEFORM 3D V6.1 via
52
53 user defined subroutine. In DEFORM, to avoid the overestimation of friction stress, the
54
55 friction stress calculated from a friction model is compared with the shear flow stress of
56
57
58
59
60
61
62
63
64
65

1
2
3
4 the deformed material at each iteration step and automatically changed to the shear flow
5 stress, if the calculated friction stress is greater than the shear flow stress.
6
7
8
9

10 11 **5.2. Friction model verification by DAE tests** 12 13

14
15
16
17 Figures 10-12 show the comparisons in the lengths of the extrudates between the DAE
18 experiments and FEM simulations. In these figures, the FEM predictions of the extrudate
19 lengths with the use of ASFM are superimposed onto the experimental data. At different
20 temperatures, the extrudates from the 2 mm bearing are longer than those from the 6 mm
21 bearing. The length difference of the extrudates increases with increasing ram
22 displacement. At the initial stage of the DAE, the workpiece is extruded at the same
23 extrusion speed in both of the dies. As the ram displacement increases, the friction force
24 increases at the same rate in the two dies due to the increasing contact area. When the
25 extrudate lengths are greater than 2 mm, the contact area in the 2 mm bearing cannot be
26 further increased. Thus a constant friction force is achieved in the 2 mm bearing. In the 6
27 mm bearing, however, the contact area is further increased due to the increase of the
28 extrudate length, thus the friction force increases and the material flow in the 6 mm
29 bearing is restricted, consequently the extrusion speed slows down. In the meanwhile, the
30 rate-dependant property of the billet material becomes explicit. In the severe deformation
31 zone of the 2 mm bearing, the material is enhanced due to the higher extrusion speed and
32 becomes more difficult to be deformed. In the severe deformation zone of the 6 mm
33 bearing, however, the low extrusion speed results in lower material strength, thus the
34 material becomes easier to be extruded. As such, a dynamic balance is maintained
35
36
37
38
39
40
41
42
43
44
45
46
47
48
49
50
51
52
53
54
55
56
57
58
59
60
61
62
63
64
65

1
2
3
4 throughout the DAE process: the friction between extrudates and bearing surfaces
5
6 increases the length difference of the extrudates; on the other hand, the effect of rate-
7
8 dependent material behaviour decreases the length difference. As can be seen from the
9
10 figures, at these three extrusion temperatures, the implementation of the ASFM has led to
11
12 highly accurate predictions, in terms of the extrudate lengths, suggesting that the ASFM
13
14 is able to represent the friction conditions at the extrudate/bearing interface.
15
16
17
18
19
20

21 Figure 13 shows the FEM predicted and experimentally obtained steady-state extrusion
22
23 forces at different extrusion temperatures. The extrusion force decreases with increasing
24
25 temperature due to the material softening at higher temperatures. It can be seen that
26
27 predictions from the ASFM show the same trend as the experimental results in terms of
28
29 the temperature effect on the extrusion force. The predictions from the ASFM achieved a
30
31 very good agreement with experimental results.
32
33
34
35
36
37
38
39

40 **6. Conclusions**

41
42
43
44 In this study, a physically based friction model (ASFM) was developed and implemented
45
46 into the FE simulation of hot aluminium extrusion process. Good agreements between the
47
48 FE simulations and experiments were achieved, in terms of extrudate length and steady
49
50 state extrusion force, indicating that ball-on-disc tests can represent the friction
51
52 conditions in the bearing channel of the hot aluminium extrusion dies. The tribological
53
54 conditions of hot aluminium extrusion process cannot be reflected by using one single
55
56 friction testing technique, and a combination of different friction testing techniques
57
58
59
60
61
62
63
64
65

1
2
3
4 should be used. For the bearing channel of the hot aluminium extrusion dies, the short
5
6 sliding distance ball-on-disc test is recommended, with the disc made from the workpiece
7
8 material and ball made from the die material. Strong adhesive friction occurs between the
9
10 hot aluminium and steel and the nature of friction in the bearing channel can be
11
12 summarized as a pressure dependant process, *i.e.* formation of isolated adhesive junctions,
13
14 adhesive junctions growth and coalescence of adhesive junctions.
15
16
17
18
19
20

21 References

22
23
24 [1] Buschhausen A, Weinmann K, Lee JY, Altan T. Evaluation of lubrication and friction
25 in cold forging using a double backward-extrusion process. Journal of materials
26 processing technology. 1992;33:95-108.
27

28 [2] Nakamura T, Bay N, Zhang ZL. FEM simulation of friction testing method based on
29 combined forward rod-backward can extrusion. J Tribol-Trans ASME. 1997;119:501-6.
30

31 [3] Nakamura T, Bay N, Zhang ZL. FEM simulation of a friction testing method based on
32 combined forward conical can-backward straight can extrusion. J Tribol-Trans ASME.
33 1998;120:716-23.
34
35

36 [4] Bakhshi-Jooybari M. A theoretical and experimental study of friction in metal
37 forming by the use of the forward extrusion process. Journal of materials processing
38 technology. 2002;125-126:369-74.
39
40

41 [5] Flitta I, Sheppard T. Nature of friction in extrusion process and its effect on material
42 flow. Mater Sci Technol. 2003;19:837-46.
43

44 [6] Abtahi S. Interface mechanisms on the bearing surface in extrusion. Sixth
45 International Aluminium Extrusion. Michigan, USA1996. p. 125-31.
46
47

48 [7] Tverlid S. Modelling of friction in the bearing channel of dies for extrusion of
49 aluminium sections. 1997;PhD thesis.
50

51 [8] Saha PK. Thermodynamics and tribology in aluminum extrusion. Wear.
52 1998;218:179-90.
53
54

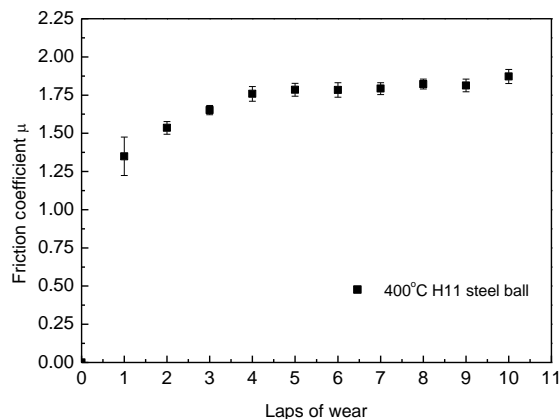
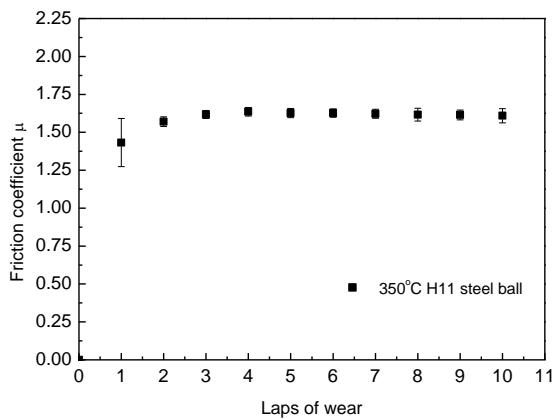
55 [9] Welo TA, S.; Skauvik, I.; Støren, S.; Melander, M.; Tjøtta, S. Friction in the bearing
56 channel of aluminium extrusion dies. 15th Riso International Symposium on Materials
57 Science. Roskilde, Denmark 1994. p. 615-20.
58
59
60
61

- 1
2
3
4 [10] Tercej M, Smolej A, Fajfar P, Turk R. Laboratory assessment of wear on nitrided
5 surfaces of dies for hot extrusion of aluminium. Tribol Int. 2007;40:374-84.
6
7
8 [11] Björk T, Bergstrom J, Hogmark S. Tribological simulation of aluminum hot
9 extrusion. Wear. 1999;224:216-25.
10
11 [12] Wang L, Zhou J, Duszczyk J. Friction in double action extrusion. Key Engineering
12 Materials 2010;424:153-60.
13
14 [13] Wang L, He Y, Zhang Y, Cai J, Zhou J, Duszczyk J, et al. Modeling of double
15 action extrusion-A novel extrusion process for friction characterization at the billet-die
16 bearing interface. Tribol Int. 2010;43:2084-91.
17
18
19 [14] Olsson M, Soderberg S, Jacobson S, Hogmark S. Simulation of cutting-tool wear by
20 a modified pin-on-disc test. Int J Mach Tools Manuf. 1989;29:377-90.
21
22
23 [15] Rech J, Claudin C, D'Eramo E. Identification of a friction model--Application to the
24 context of dry cutting of an AISI 1045 annealed steel with a TiN-coated carbide tool.
25 Tribol Int. 2009;42:738-44.
26
27 [16] Bonnet C, Valiorgue F, Rech J, Claudin C, Hamdi H, Bergheau JM, et al.
28 Identification of a friction model--Application to the context of dry cutting of an AISI
29 316L austenitic stainless steel with a TiN coated carbide tool. International Journal of
30 Machine Tools and Manufacture. 2008;48:1211-23.
31
32
33 [17] Zemzemi F, Rech J, Ben Salem W, Dogui A, Kapsa P. Identification of a friction
34 model at tool/chip/workpiece interfaces in dry machining of AISI4142 treated steels.
35 Journal of materials processing technology. 2009;209:3978-90.
36
37
38 [18] Ranganatha S, Kailas SV, Storen S, Srivatsan TS. Role of temperature on sliding
39 response of aluminum on steel of a hot extrusion. Mater Manuf Process. 2008;23:29-36.
40
41
42 [19] Wang LL, Cai JQ, Zhou J, Duszczyk J. Characteristics of the Friction Between
43 Aluminium and Steel at Elevated Temperatures During Ball-on-Disc Tests. Tribology
44 Letters. 2009;36:183-90.
45
46
47 [20] Wang L, He Y, Zhou J, Duszczyk J. Effect of temperature on the frictional
48 behaviour of an aluminium alloy sliding against steel during ball-on-disc tests. Tribol Int.
49 2010;43:299-306.
50
51
52 [21] Bay N, Olsson DD, Andreasen JL. Lubricant test methods for sheet metal forming.
53 Tribol Int. 2008;41:844-53.
54
55 [22] Tan XC, Bay N, Zhang WQ. On parameters affecting metal flow and friction in the
56 double cup extrusion test. Scand J Metall. 1998;27:246-52.
57
58
59
60
61
62
63
64
65

- 1
2
3
4 [23] Schrader T, Shirgaokar M, Altan T. A critical evaluation of the double cup extrusion
5 test for selection of cold forging lubricants. *Journal of materials processing technology*.
6 2007;189:36-44.
7
8
9 [24] Shirzadi AA, Assadi H, Wallach ER. Interface evolution and bond strength when
10 diffusion bonding materials with stable oxide films. *Surf Interface Anal*. 2001;31:609-18.
11
12 [25] Jiang J, Arnell RD, Dixit G. The influence of ball size on tribological behaviour of
13 MoS₂ coating tested on a ball-on-disk wear rig. *Wear*. 2000;243:1-5.
14
15 [26] Hegadekatte V, Huber N, Kraft O. Modeling and simulation of wear in a pin on disc
16 tribometer. *Tribology Letters*. 2006;24:51-60.
17
18 [27] Schey JA. *Tribology in metalworking : friction, lubrication, and wear*. Metals Park,
19 Ohio: American Society for Metals; 1983.
20
21 [28] Wang L, He Y, Zhou J, Duszczek J. Modelling of plowing and shear friction
22 coefficients during high-temperature ball-on-disc tests. *Tribol Int*. 2009;42:15-22.
23
24 [29] Riahi AR, Alpas AT. Adhesion of AA5182 aluminum sheet to DLC and TiN
25 coatings at 25 degrees C and 420 degrees C. *Surf Coat Technol*. 2007;202:1055-61.
26
27 [30] Riahi AR, Edrisy A, Alpas AT. Effect of magnesium content on the high
28 temperature adhesion of Al-Mg alloys to steel surfaces. *Surf Coat Technol*.
29 2009;203:2030-5.
30
31 [31] Bowden FP, Tabor D. *The friction and lubrication of solids*. Oxford,: Clarendon
32 Press; 1950.
33
34 [32] Hutchings IM. *Tribology : friction and wear of engineering materials*. Boca Raton:
35 CRC Press; 1992.
36
37 [33] Bhushan B. *Introduction to tribology*. New York: John Wiley & Sons; 2002.
38
39 [34] Björk T, Westergård R, Hogmark S. Wear of surface treated dies for aluminium
40 extrusion -- a case study. *Wear*. 2001;249:316-23.
41
42 [35] Björk T, Westergård R, Hogmark S, Bergström J, Hedenqvist P. Physical vapour
43 deposition duplex coatings for aluminium extrusion dies. *Wear*. 1999;225-229:1123-30.
44
45 [36] Gutovskaya J, Solberg JK, Lange HI, Andersen LH. Wear of Inconel 718 die during
46 aluminium extrusion--a case study. *Wear*. 2004;256:126-32.
47
48 [37] Kong TF, Chan LC, Lee TC. Experimental Study of Effects of Process Parameters in
49 Forge-Welding Bimetallic Materials: AISI 316L Stainless Steel and 6063 Aluminium
50 Alloy. *Strain*. 2009;45:373-9.
51
52
53
54
55
56
57
58
59
60
61
62
63
64
65

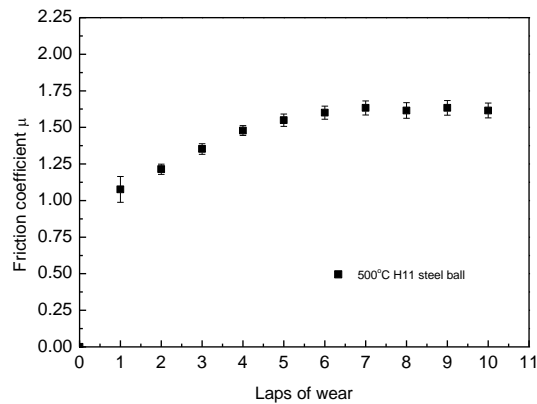
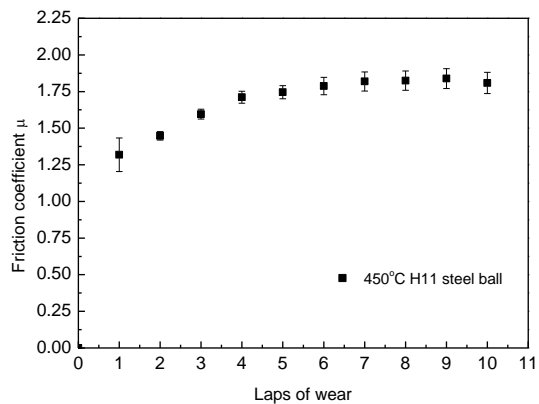
- 1
2
3
4 [38] Kong TF, Chan LC, Lee TC. Weld Diffusion Analysis of Forming Bimetallic
5 Components Using Statistical Experimental Methods. Mater Manuf Process.
6 2009;24:422-30.
7
8
9 [39] Sahin M. Joining of stainless-steel and aluminium materials by friction welding. Int
10 J Adv Manuf Technol. 2009;41:487-97.
11
12 [40] Ma X, de Rooij M, Schipper D. A load dependent friction model for fully plastic
13 contact conditions. Wear. 2010;269:790-6.
14
15 [41] Ma X. Surface quality of aluminium extrusion products [PhD thesis]: PhD thesis,
16 Twente University; 2011.
17
18 [42] Rooij MBd. Tribological aspects of unlubricated deepdrawing processes [PhD]: PhD
19 thesis, Twente University; 1998.
20
21 [43] Schedin E, Lehtinen B. Galling mechanisms in lubricated systems: A study of sheet
22 metal forming. Wear. 1993;170:119-30.
23
24 [44] Schedin E. Galling mechanisms in sheet forming operations. Wear. 1994;179:123-8.
25
26 [45] Roizard X, Vonstebut J, Paintendre B, Venumiere L, Int Deep Drawing Res GRP.
27 The influence of contact temperature on metal transfer and galling in strip drawing. Sheet
28 Metals in Forming Processes : Congress Proceedings: 16th Biennial Congress Iddrg.
29 1992:161-71.
30
31 [46] Ghosh M, Bhanumurthy K, Kale GB, Krishnan J, Chatterjee S. Diffusion bonding of
32 titanium to 304 stainless steel. Journal of Nuclear Materials. 2003;322:235-41.
33
34 [47] Moufki A, Molinari A, Dudzinski D. Modelling of orthogonal cutting with a
35 temperature dependent friction law. Journal of the Mechanics and Physics of Solids.
36 1998;46:2103-38.
37
38 [48] Wang L, He Y, Zhang Y, Cai J, Zhou J, Duszczyc J, et al. Modeling of double
39 action extrusion - a novel extrusion process for friction characterization at the billet-die
40 bearing interface. Tribol Int. 2010;In press.
41
42 [49] Pluijms GJ. Flow Stress Characterization of Aluminum Alloys in Warm and Hot
43 Working Conditions [Master's thesis]. Delft: Master's thesis of Delft University of
44 Technology; 2008.
45
46
47
48
49
50
51
52
53
54
55
56
57
58
59
60
61
62
63
64
65

1
2
3
4
5
6
7
8
9
10
11
12
13
14
15
16
17
18
19
20
21
22
23
24
25
26
27
28
29
30
31
32
33
34
35
36
37
38
39
40
41
42
43
44
45
46
47
48
49
50
51
52
53
54
55
56
57
58
59
60
61
62
63
64
65



(a)

(b)



(c)

(d)

Figure 1 Evolution of the friction coefficient with increasing sliding distance at different temperatures.

1
2
3
4
5
6
7
8
9
10
11
12
13
14
15
16
17
18
19
20
21
22
23
24
25
26
27
28
29
30
31
32
33
34
35
36
37
38
39
40
41
42
43
44
45
46
47
48
49
50
51
52
53
54
55
56
57
58
59
60
61
62
63
64
65

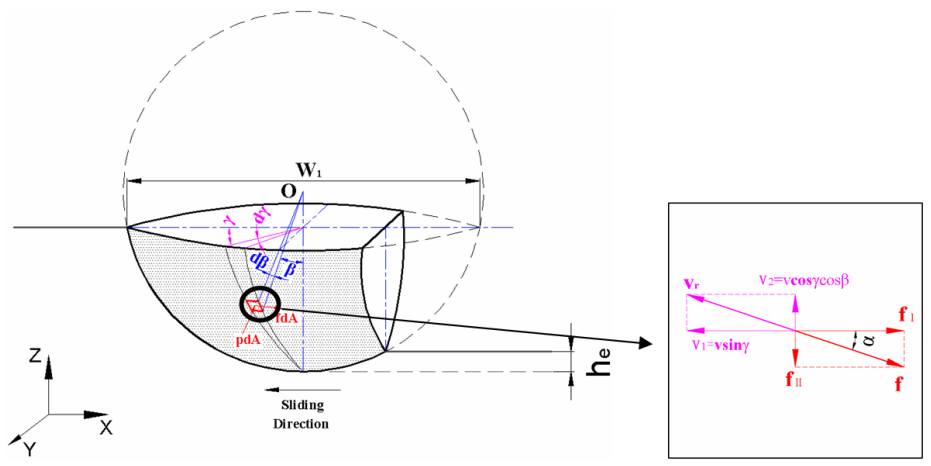


Figure 2 Close-up view of the friction force and velocity on an elemental area

1
2
3
4
5
6
7
8
9
10
11
12
13
14
15
16
17
18
19
20
21
22
23
24
25
26
27
28
29
30
31
32
33
34
35
36
37
38
39
40
41
42
43
44
45
46
47
48
49
50
51
52
53
54
55
56
57
58
59
60
61
62
63
64
65

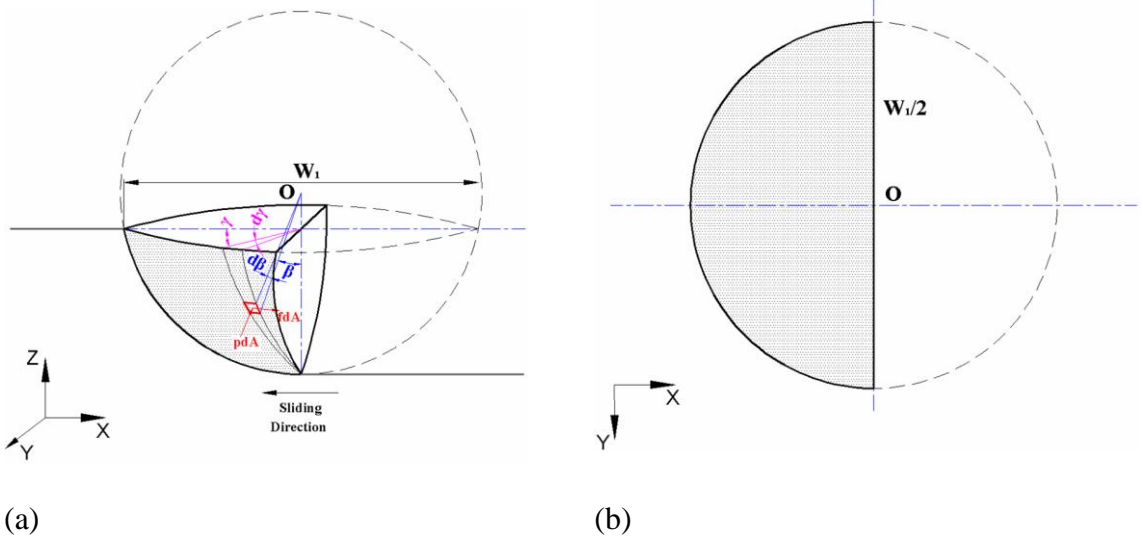


Figure 3 Schematic drawing of the contact interface in the first lap of wear during ball-on-disc testing

1
2
3
4
5
6
7
8
9
10
11
12
13
14
15
16
17
18
19
20
21
22
23
24
25
26
27
28
29
30
31
32
33
34
35
36
37
38
39
40
41
42
43
44
45
46
47
48
49
50
51
52
53
54
55
56
57
58
59
60
61
62
63
64
65

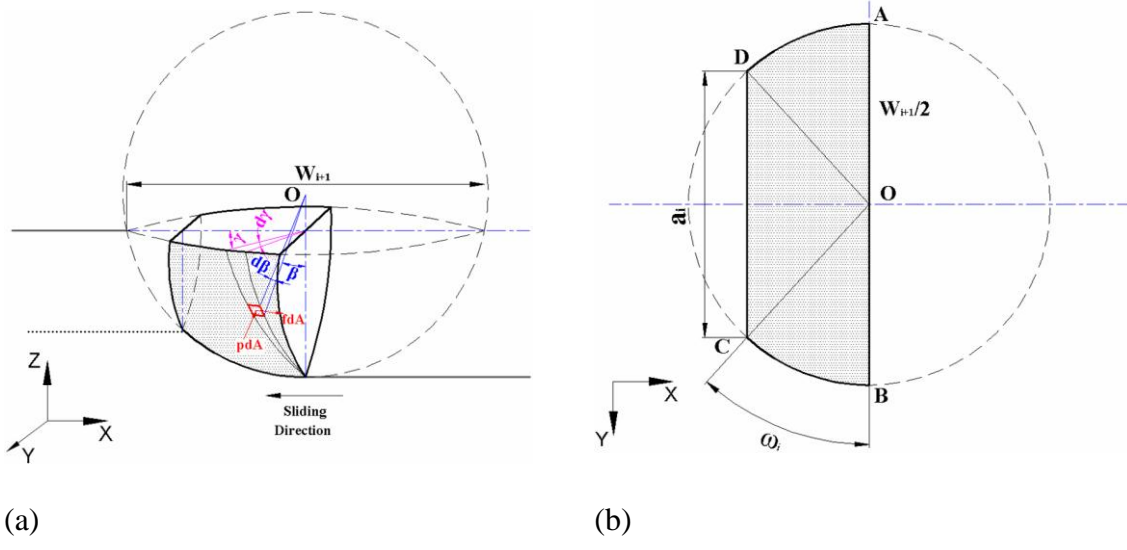


Figure 4 Schematic drawing of the contact interface in an arbitrary $(i+1)th$ lap of wear during ball-on-disc testing

1
2
3
4
5
6
7
8
9
10
11
12
13
14
15
16
17
18
19
20
21
22
23
24
25
26
27
28
29
30
31
32
33
34
35
36
37
38
39
40
41
42
43
44
45
46
47
48
49
50
51
52
53
54
55
56
57
58
59
60
61
62
63
64
65

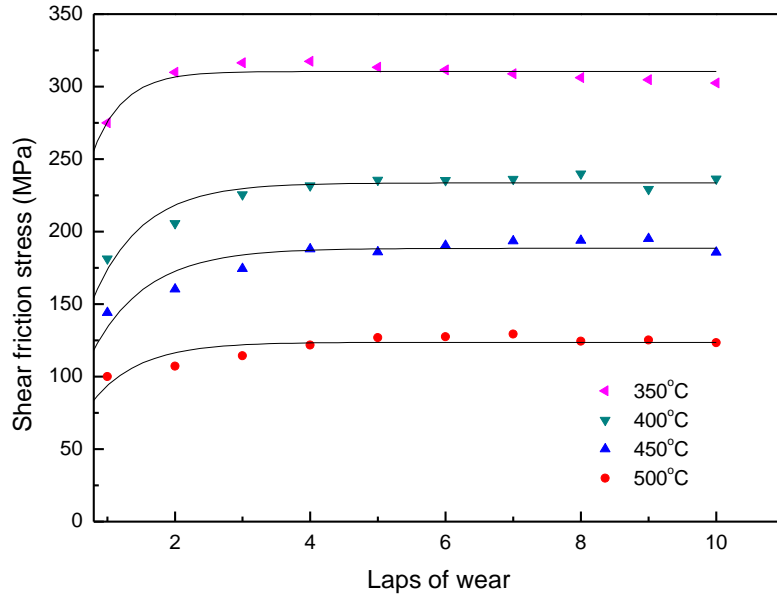


Figure 5 Evolution of the shear friction stress with sliding distance.

1
2
3
4
5
6
7
8
9
10
11
12
13
14
15
16
17
18
19
20
21
22
23
24
25
26
27
28
29
30
31
32
33
34
35
36
37
38
39
40
41
42
43
44
45
46
47
48
49
50
51
52
53
54
55
56
57
58
59
60
61
62
63
64
65

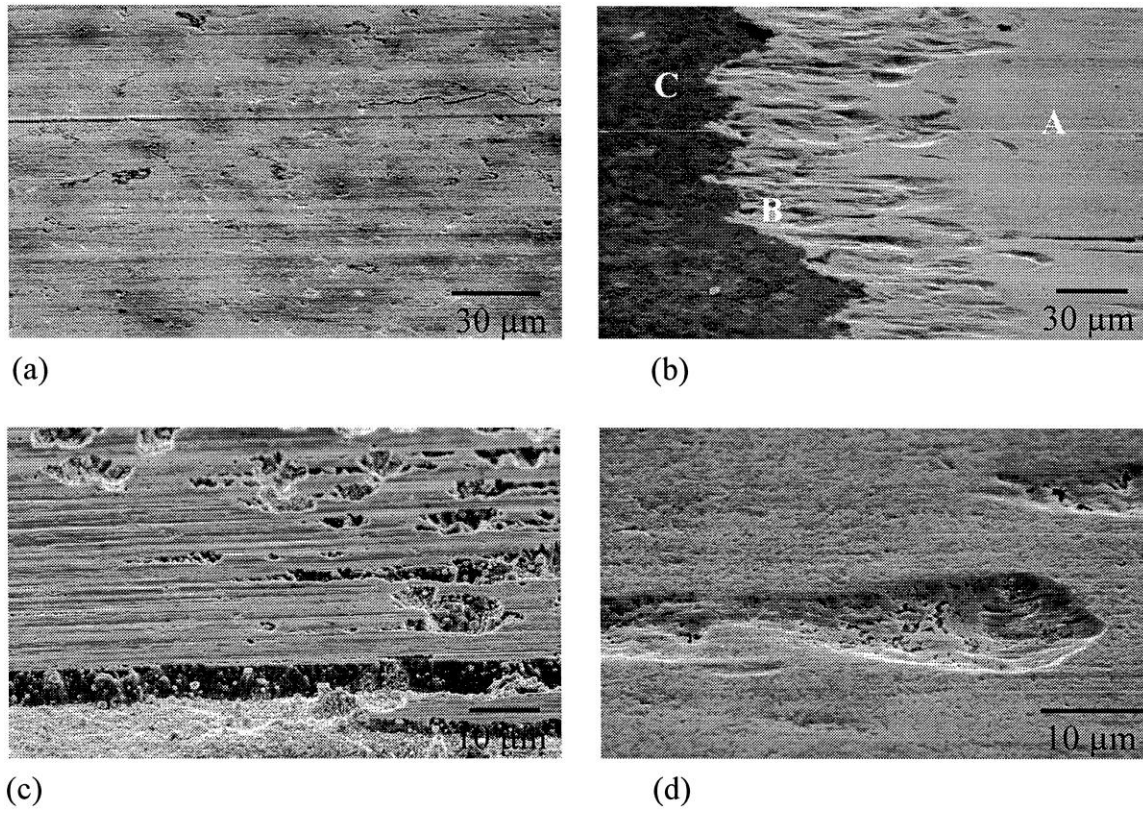


Figure 6 (a) Exposed steel substrate in the sticking zone at A in (b). (b) A transition zone, at B in (b), observed between slipping zone at C in (b), and sticking zone at A in (b). (c) Partly disrupted compound layer in the transition zone at B in (b). (d) Isolated local wear pit in the slipping zone observed at C in (b) [11]

1
2
3
4
5
6
7
8
9
10
11
12
13
14
15
16
17
18
19
20
21
22
23
24
25
26
27
28
29
30
31
32
33
34
35
36
37
38
39
40
41
42
43
44
45
46
47
48
49
50
51
52
53
54
55
56
57
58
59
60
61
62
63
64
65

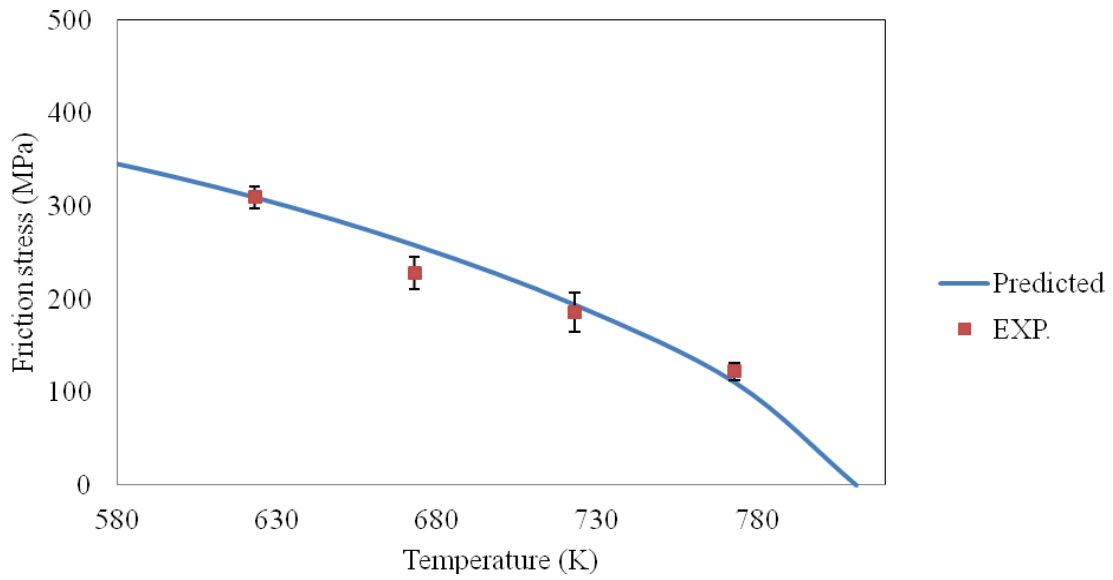


Figure 7 Evolution of friction stress between AA7475 and H11 steel at different temperatures

1
2
3
4
5
6
7
8
9
10
11
12
13
14
15
16
17
18
19
20
21
22
23
24
25
26
27
28
29
30
31
32
33
34
35
36
37
38
39
40
41
42
43
44
45
46
47
48
49
50
51
52
53
54
55
56
57
58
59
60
61
62
63
64
65

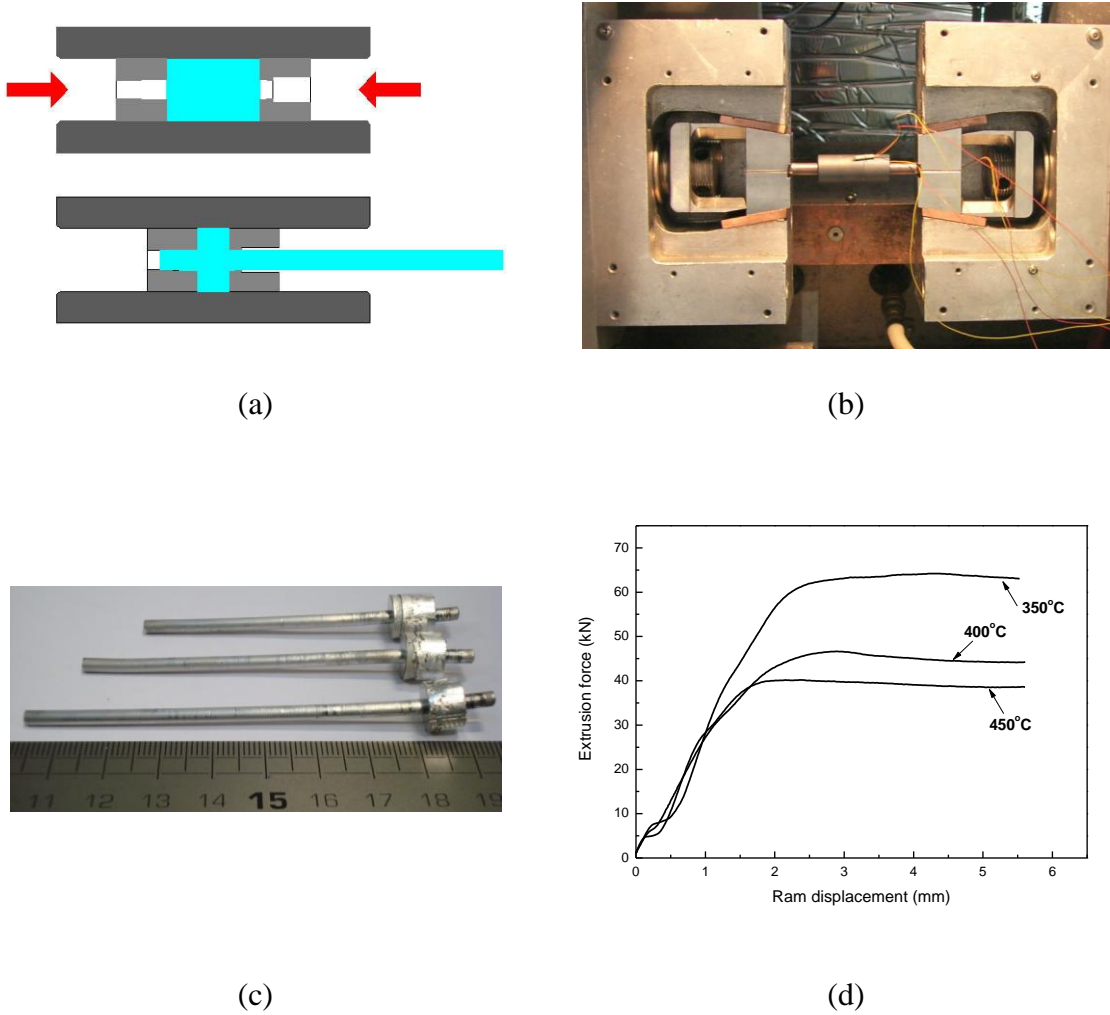


Figure 8 The (a) principle, (b) experimental setup and (c and d) typical test results of DAE

1
2
3
4
5
6
7
8
9
10
11
12
13
14
15
16
17
18
19
20
21
22
23
24
25
26
27
28
29
30
31
32
33
34
35
36
37
38
39
40
41
42
43
44
45
46
47
48
49
50
51
52
53
54
55
56
57
58
59
60
61
62
63
64
65

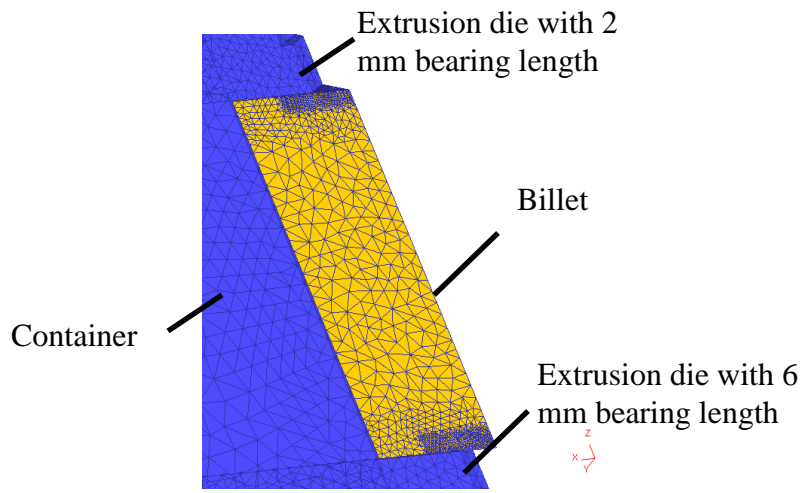


Figure 9 FE model for the DAE

1
2
3
4
5
6
7
8
9
10
11
12
13
14
15
16
17
18
19
20
21
22
23
24
25
26
27
28
29
30
31
32
33
34
35
36
37
38
39
40
41
42
43
44
45
46
47
48
49
50
51
52
53
54
55
56
57
58
59
60
61
62
63
64
65

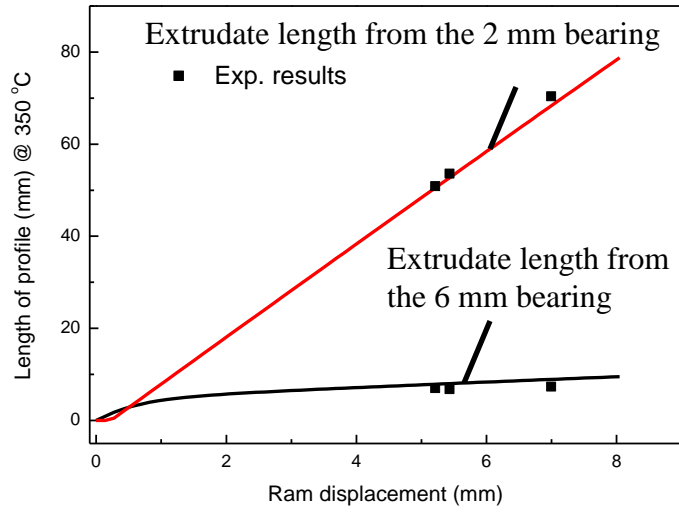


Figure 10 Comparison in the extrudate lengths from DAE at 350°C between the experiments and FEM simulations.

1
2
3
4
5
6
7
8
9
10
11
12
13
14
15
16
17
18
19
20
21
22
23
24
25
26
27
28
29
30
31
32
33
34
35
36
37
38
39
40
41
42
43
44
45
46
47
48
49
50
51
52
53
54
55
56
57
58
59
60
61
62
63
64
65

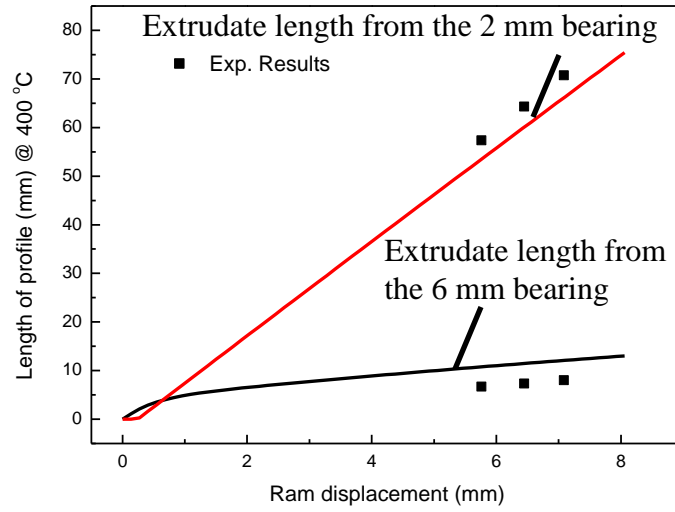


Figure 11 Comparison in the extrudate lengths from DAE at 400°C between the experiments and FEM simulations.

1
2
3
4
5
6
7
8
9
10
11
12
13
14
15
16
17
18
19
20
21
22
23
24
25
26
27
28
29
30
31
32
33
34
35
36
37
38
39
40
41
42
43
44
45
46
47
48
49
50
51
52
53
54
55
56
57
58
59
60
61
62
63
64
65

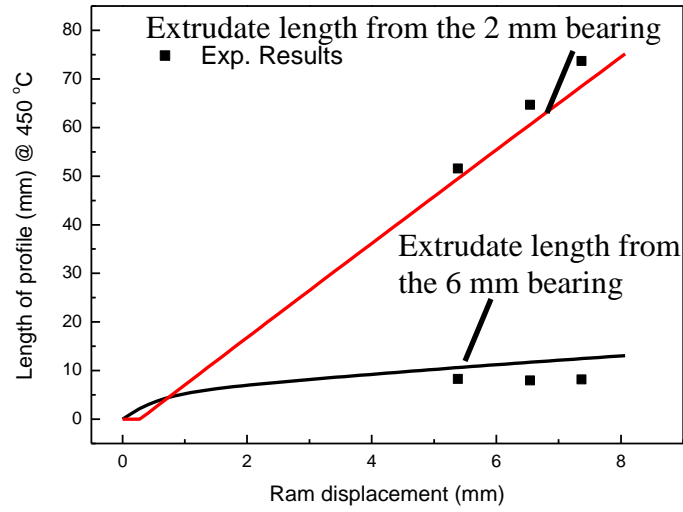


Figure 12 Comparison in the extrudate lengths from DAE at 450°C between the experiments and FEM simulations.

1
2
3
4
5
6
7
8
9
10
11
12
13
14
15
16
17
18
19
20
21
22
23
24
25
26
27
28
29
30
31
32
33
34
35
36
37
38
39
40
41
42
43
44
45
46
47
48
49
50
51
52
53
54
55
56
57
58
59
60
61
62
63
64
65

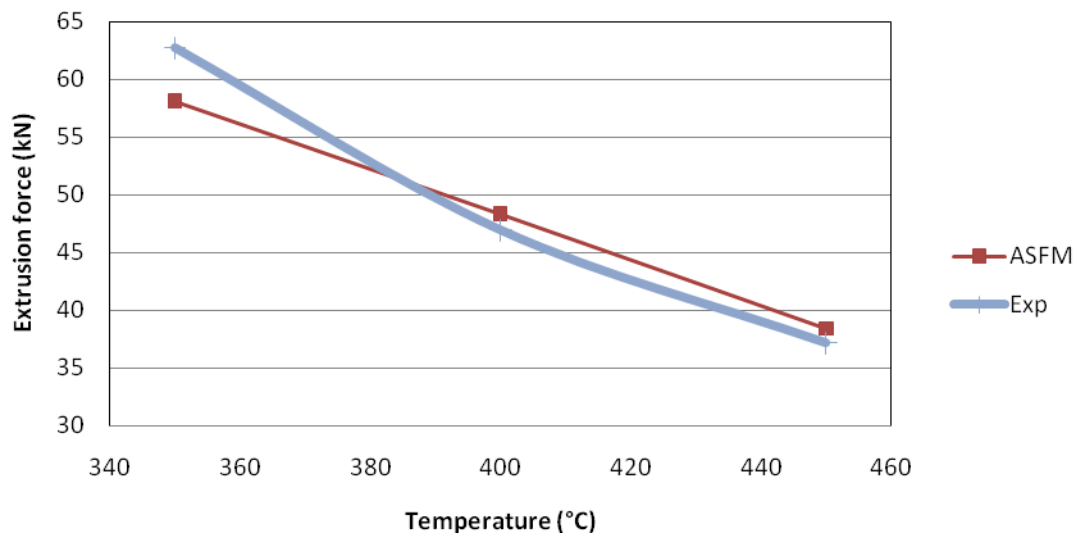


Figure 13 Steady state extrusion forces at different extrusion temperatures